# Identification of growth regulators using cross-species network analysis in plants

Pasquale Luca Curci[1,2,3], Jie Zhang[1,2+], Niklas Mähler[4+], Carolin Seyfferth[1,2,4], Chanaka Mannapperuma[4], Tim Diels[1,2], Tom Van Hautegem[1,2], David Jonsen[6], Nathaniel Street[4], Torgeir R. Hvidsten[4,7], Magnus Hertzberg[6], Ove Nilsson[5], Dirk Inze[1,2], Hilde Nelissen[1,2], Klaas Vandepoele[1,2,8*]

(1) Department of Plant Biotechnology and Bioinformatics, Ghent University, Technologiepark 71, 9052 Ghent, Belgium

(2) VIB Center for Plant Systems Biology, Technologiepark 71, 9052 Ghent, Belgium

(3) Institute of Biosciences and Bioresources, National Research Council (CNR), Via Amendola 165/A, 70126 Bari, Italy

(4) Umea Plant Science Centre (UPSC), Department of Plant Physiology, Umeå University, 90187 Umeå, Sweden.

(5) Umea Plant Science Centre (UPSC), Department of Forest Genetics and Plant Physiology, Swedish University of Agricultural Sciences, 90183 Umeå, Sweden.

(6) SweTree Technologies AB, Skogsmarksgränd 7, SE-907 36 Umeå, Sweden

(7) Faculty of Chemistry, Biotechnology and Food Science, Norwegian University of Life Sciences, 1432 Ås, Norway

(8) Bioinformatics Institute Ghent, Ghent University, Technologiepark 71, 9052 Ghent, Belgium

+ both authors contributed equally

* Corresponding author: Klaas.Vandepoele@psb.vib-ugent.be

**Short title**: Identification of growth regulators in plants

**Author contributions**: P.L.C., N.S., T.R.H., H.N., O.N., D.I. and K.V. designed the research; P.L.C., J.Z., N.M., C.S., C.M., T.D., and T.V.H. performed research and data analysis; N.M., T.V.H., D.J., and M.H. contributed data and analytic tools, P.L.C., J.Z. and K.V. wrote the paper with input from all co-authors.

**One-sentence summary**: Cross-species network analysis enables identification and validation of growth regulators in Arabidopsis.

The author responsible for distribution of materials integral to the findings presented in this article in accordance with the policy described in the Instructions for Authors (https://academic.oup.com/pphys/pages/General-Instructions) is Klaas Vandepoele.


## Abstract

With the need to increase plant productivity, one of the challenges plant scientists are facing is to identify genes that play a role in beneficial plant traits. Moreover, even when such genes are found, it is generally not trivial to transfer this knowledge about gene function across species to identify functional orthologs. Here, we focused on the leaf to study plant growth. First, we built leaf growth transcriptional networks in Arabidopsis (*Arabidopsis thaliana*), maize (*Zea mays*), and aspen (*Populus tremula*). Next, known growth regulators, here defined as genes that when mutated or ectopically expressed alter plant growth, together with cross-species conserved networks, were used as guides to predict novel Arabidopsis growth regulators. Using an in-depth literature screening, 34 out of 100 top predicted growth regulators were confirmed to affect leaf phenotype when mutated or overexpressed and thus represent novel potential growth regulators. Globally, these growth regulators were involved in cell cycle, plant defense responses, gibberellin, auxin, and brassinosteroid signaling. Phenotypic characterization of loss-of-function lines confirmed two predicted growth regulators to be involved in leaf growth (*NPF6.4* and *LATE MERISTEM IDENTITY2*). In conclusion, the presented network approach offers an integrative cross-species strategy to identify genes involved in plant growth and development.


## Introduction

The need to increase plant productivity reveals that, despite the detailed information gained on plant genomes, modelling plant growth and translating the molecular knowledge obtained in model plant species to crops is not trivial (Nuccio et al., 2018; Simmons et al., 2021, Inze and Nelissen, 2022). Plant organ growth is one of the processes that is well-studied in model plants (Vercruysse et al., 2020a), playing a major role in affecting plant productivity (Sun et al., 2017). New plant organs are formed and then grow continuously throughout development. Upon adverse conditions,

growth adjustments are among the first plant responses, rendering growth regulation an important yield component (Gray and Brady, 2016; Nowicka, 2019). The growth of plants involves complex mechanisms controlling processes from the cellular to the whole-organism level (Verbraeken et al., 2021). However, which growth zones or cell types are most important in controlling organ growth is not always clear.

Numerous genes, which we refer to as growth regulators, have been identified that when mutated or ectopically expressed alter organ size, such as leaf size, in plants. Detailed transcriptome and functional analyses have revealed that many of these genes are part of functional modules conserved across plant species (Vercruysse et al., 2020b). Previous research has shown that largely similar cellular and molecular pathways govern the fundamental growth processes in dicots and monocots (Anastasiou et al., 2007; Nelissen et al., 2016). This observation is based on the presence of functionally conserved orthologous growth regulators which promote organ growth in both dicots and monocots. Notable examples are genes encoding CYTOCHROME P450, FAMILY 78, SUBFAMILY A, POLYPEPTIDE 8 (CYP78A), AUXIN-REGULATED GENE INVOLVED IN ORGAN SIZE (ARGOS), rate limiting GA biosynthesis enzymes, BRASSINOSTEROID INSENSITIVE 1 (BRI1), ANGUSTIFOLIA3 and GROWTH-REGULATING FACTORS (Powell and Lenhard, 2012; Vercruysse et al., 2020a).

The complex and highly dynamic nature of the regulatory networks controlling complex traits makes the identification of growth regulatory genes challenging (Baxter, 2020). Moreover, duplication events across the plant kingdom have caused a general enlargement of gene families and, with it, plant- and tissue-specific functional specialization (Jones and Vandepoele, 2020). It became clear that, even when the gene space is well characterized and conserved, the translation from model species to crops is not straightforward (Gong et al., 2022; Inze and Nelissen, 2022). One of the bottlenecks lies in the complexity of crop genomes, such as polyploidy, and the subsequent difficulty in identifying functional orthologs.

Gene orthology information is essential to transfer functional annotations from model plants with high-quality annotations (e.g. *Arabidopsis thaliana*) to other species. Functional annotations derived from experimental evidence can be used to identify relevant orthologs and drive gene function discovery in crops (Lee et al., 2015, 2019). This approach is not straightforward, mainly for two reasons: first, the orthology approach normally leads to the identification of complex (one-

to-one, one-to-many and many-to-many) orthology relationships (Movahedi et al., 2011; Van Bel et al., 2012); second, for genes with multiple orthologs, it has been observed that the ortholog with the highest protein sequence similarity is often not the ortholog with the most similar regulation, indicating that identifying functionally conserved orthologs is challenging (Patel et al., 2012; Netotea et al., 2014).

Biological networks offer the means to study the complex organization of gene interactions. Densely connected network clusters form gene modules, defined as groups of linked genes with similar expression profiles (i.e. co-expressed genes), which also tend to be co-regulated and functionally related (Heyndrickx and Vandepoele, 2012; Klie et al., 2012). Although transferring network links from better annotated species to crops is the most intuitive approach and has proven to be helpful (Ficklin and Feltus, 2011; Obertello et al., 2015), it has been shown that only ~20-40% of the co-expression links are conserved in pairwise comparison of Arabidopsis (*Arabidopsis thaliana*), *Populus*, and rice (*Oryza sativa*) (Netotea et al., 2014). On the other hand, it has been shown that using gene modules that are conserved across species can increase the amount of biological knowledge transferred from one species to another (Mutwil et al., 2011; Heyndrickx and Vandepoele, 2012; Cheng et al., 2021). Such conserved gene modules mirror biological processes conserved across species, meaning that the orthologous genes present in these modules are involved in the same process and potentially perform the same function (Stuart et al., 2003; Ruprecht et al., 2011). Significantly conserved cross-species modules (with many shared orthologs) can be used to transfer gene function annotations and analyze expression conservation for paralogs involved in complex many-to-many orthology relationships. A guilt-by-association approach can also then be used to infer functions of unknown genes from the functions of co-expressed annotated genes (Wolfe et al., 2005; Lee et al., 2010; De Smet and Marchal, 2010; Klie et al., 2012; Rhee and Mutwil, 2014).

Here, we aimed at developing an integrative approach to identify functionally conserved regulators, leveraging high-resolution transcriptomes and the power of cross-species network biology. In particular, we chose leaf as a system to study plant growth, as high-quality datasets covering cell proliferation and expansion are available in three plant species: two dicotyledonous plants, the annual plant Arabidopsis and the perennial plant aspen (*Populus tremula*), and one monocotyledonous plant, maize (*Zea mays*). We leveraged these data to construct aggregated gene

networks for each species and identified, through gene neighborhood conservation analysis, genes with cross-species network conservation. Subsequently, we used known plant growth regulators, belonging to various functional modules and influencing growth of different plant organs, as guide genes to predict putative growth regulators among these conserved genes. For the top 100 predicted growth regulators, we screened the literature to investigate if predictions linked to leaf growth were obtained. For a subset of highly ranked predictions with no reported information on plant growth, we performed phenotypic analyses and succeeded in validating two novel Arabidopsis growth regulators.

## Results

### Network construction and gene neighborhood conservation analysis

To perform network construction based on gene expression information, we used transcriptomic data from leaves, which were selected as a representative system to study plant growth. This choice was primarily motivated by the well-known similarities in leaf growth regulation across dicots and monocots, which make cross-species comparison of gene networks straightforward and useful for gene function discovery (Vercruysse et al., 2020b). Secondly, our motivation relied on the availability of large-scale expression profiling studies, which allow selecting similar samples and constructing a congruent dataset for the different species. Expression compendia were built for Arabidopsis, maize and aspen that contained a minimum of 24 leaf samples (Figure 1, step 1; Supplemental Table S1; Supplemental Methods). These expression compendia all include developmental stages with active cell proliferation and cell expansion. The Arabidopsis expression compendium was composed of three main developmental phases: cell proliferation, cell expansion and the transition between these two phases. For maize, the developmental expression compendium included a newly generated high-resolution dataset and covered cell proliferation, cell expansion and mature phases of development (Supplemental Methods). For aspen, samples covered the developmental stages ranging from the very youngest leaf primordia to fully expanded and mature leaves. In total, expression data covered 20,313 genes for Arabidopsis, 29,383 genes for maize, and 35,309 genes for aspen (Supplemental Dataset S1).

The network construction was performed for each species with Seidr, a toolkit to perform multiple gene network inferences and combine their results into a unified meta-network (Schiffthaler et al.,

2018). For each network inference algorithm included, a fully connected weighted gene network was constructed. These were in turn aggregated into a weighted meta-network (simply "network" hereinafter, Figure 1, step 2). When applying a weight threshold, the network density was defined as the ratio between the number of links with a weight higher than this threshold and the number of links in the weighted network. To dissect the network structure, several thresholds were used to subset the networks into more stringent density subnetworks (DSs). For each species network, five DSs were obtained ranging from DS1 (top 0.1% links) with an average of 358,455 links, to DS5 (top 10% links) with an average of 35,845,512 links (Figure 1, step 3), with higher densities corresponding to a higher number of neighbors for each gene in the network (Supplemental Figure S1). A gene's neighborhood is defined as all genes connected with this gene for a given network.

Genes showing gene neighborhood conservation across species are part of conserved functional modules controlling distinct biological processes. This implies that the conserved network containing these genes confers a selective advantage and therefore that these genes are functionally related (Stuart et al., 2003). However, which gene neighborhood size to select to identify conserved growth-related functional modules is not straightforward, as being too stringent might lead to the loss of valuable interactions while being too relaxed might include non-functional interactions potentially representing noise (Movahedi et al. 2012). To identify genes showing network conservation in different species, a gene neighborhood conservation analysis was performed using each DS and the information on the orthology relationships between Arabidopsis, maize and aspen genes (Figure 1, step 4a). The network neighborhood of a gene is represented by all genes connected to it, at a given threshold. This concept was used to identify "triplets" (Supplemental Dataset S2), each containing three orthologous genes across Arabidopsis, maize and aspen with statistically significant overlaps between their gene network neighborhoods (see Methods). In an example triplet (Figure 1, step 4a), a specific Arabidopsis gene *A1*, will have an ortholog *Z1* in maize and another ortholog *P1* in aspen and these three genes will have a significant overlap of their gene network neighborhoods. Due to the complex orthology relationships that exist in plants, each gene can belong to one or multiple triplets as it can have one or more orthologs. For example, an Arabidopsis gene with only one ortholog in maize and aspen, assuming they have significant overlap of their gene network neighborhoods, will belong to one triplet. In contrast, another Arabidopsis gene with two orthologs in maize and three in aspen, assuming they also all have significant overlaps of their gene network neighborhoods, will belong to six triplets. We refer to

the set of unique genes that are part of triplets as "triplet genes". Next, the conserved gene neighborhoods were used to dissect the complex network structures of these plants and to functionally harness the orthology relationships. The cross-species networks are available in an interactive web application (https://beta-complex.plantgenie.org).

**Delineation of conserved growth regulators**

Since the output of cell proliferation and expansion are strongly contributing to leaf size, we hypothesized that the generated triplets were an excellent source to extract orthologs potentially altering plant growth, representing conserved GRs. Growth regulators typically act by stimulating cell proliferation (yielding a higher cell number, as in the case of GRF (GROWTH-REGULATING FACTOR) and GIF (GRF-INTERACTING FACTOR) proteins (Lee et al., 2009)) and/or cell expansion (as in the case of *ZHD5* (*ZINC-FINGER HOMEODOMAIN 5*) (Hong et al., 2011)). We generated a list of known GRs ("primary-GRs") covering 71 primary-GRs from Arabidopsis, 71 from aspen and eight from maize. While the Arabidopsis and maize GRs mainly have a role in controlling leaf size, the aspen GRs are affecting stem size. In both organs, cell proliferation and expansion play an important role in controlling growth (Serrano-Mislata and Sablowski, 2018). This list of genes was obtained by collecting scientific literature and by phenotypic analysis of mutant and over-expression lines in Arabidopsis, maize, and aspen. We then used the triplets to transfer GRs from maize and aspen to Arabidopsis ("translated-GRs"). In other words, primary-GRs from maize and aspen, also identified as triplet genes, were used to extract Arabidopsis orthologs with gene neighborhood conservation. The primary-GRs and translated-GRs were finally merged and filtered for high expression variation in the Arabidopsis expression compendium to retain only those active during either cell proliferation or cell expansion. The resulting set, named "expression-supported GRs" (Supplemental Table S2, Supplemental Figure S2), was composed of 82 GRs, including 24 Arabidopsis primary-GRs and 58 translated-GRs (*GRF2* and *GA20OX1* (*GIBBERELLIN 20-OXIDASE 1*) were shared between primary-GR and translated-GR sets). According to their expression profiles in Arabidopsis, 35 expression-supported GRs showed maximal expression during cell proliferation, including several proliferation marker genes like GROWTH-REGULATING FACTORs (e.g. *GRF1*, *GRF2*, *GRF3*), AINTEGUMENTA (*ANT* (Mizukami and Fischer, 2000) and *KLUH* (Anastasiou et al., 2007)), and 47 expression-supported GRs had increased expression during cell expansion, such as

*GA20Ox1* (Barboza et al., 2013) and *BR ENHANCED EXPRESSION 2* (*BEE2* (Friedrichsen et al., 2002)).

The 82 expression-supported GRs (from here on simply referred to as "GRs") represent our guide genes, obtained by the integration of prior knowledge on plant growth and the cross-species gene neighborhood conservation approach, to identify candidate GRs.

**Functional analysis of cross-species conserved networks underlying leaf cell proliferation and expansion**

To explore cross-species conserved genes that function during cell proliferation and expansion, we performed a Gene Ontology (GO (Ashburner et al., 2000)) functional enrichment analysis of the Arabidopsis triplet genes from each DS across two sets: (1) all triplet genes (All) and (2) the subset of triplet genes including the 82 GRs and their co-expressed triplet genes (Growth regulator-related triplet genes) (Figure 2). The total number of triplets ranged from 1,739 (DS1) to 243,645 (DS5) (Figure 2A; Supplemental Dataset S2). To assess the significance of these numbers, a permutation approach was employed where the orthology relationships were randomized 500 times and the number of triplets obtained from each permutation was recorded. The number of triplets observed were highly significant with not a single permutation for any DS exceeding the number of triplets observed in the non-permuted data (p-value<0.002). The number of unique Arabidopsis triplet genes ranged from 211 (DS1) to 6,526 (DS5) indicating that less sparse networks tend to have more genes and more conserved gene neighborhoods (Figure 2A). Interestingly, GRs and their network neighbors on average made up 71% of the triplet genes across the five DSs, suggesting that leaf growth-related gene networks are well conserved during leaf development across plant species. For simplicity, from here on we will refer to triplet genes at a specific DS as, for example at DS1, "genes conserved at DS1". The functional enrichment (Figure 2B) showed that triplet genes from the most stringent subnetwork (DS1) were enriched for basal biological processes during leaf development, including photosynthesis (e.g. glucose metabolic process, response to light and carbon fixation) and translation (e.g. large and small ribosomal subunits). Processes such as cell division and cell cycle regulation were significantly enriched for genes conserved at DS2 and DS3, including genes coding for cyclins (type A, B, D and P), cyclin dependent kinases (*CDK*) and their subunits (*CKS*), and other genes involved in the spindle formation (i.e. *MICROTUBULE-ASSOCIATED PROTEINS (MAP)65-4 and -5*). Cell expansion-

related processes were identified among genes conserved at DS3 and included genes coding for expansins (EXP) and xyloglucan endotransglucosylases/hydrolases (XTH). Genes conserved at the two least stringent subnetworks (DS4 and DS5) were enriched for GO terms related to cell wall organization (e.g. lignan biosynthesis, pectin degradation, lignin metabolism), defense response to biotic and abiotic stresses (e.g. defense response to oomycetes, response to salt stress and heat stress), and transmembrane transport and hormone signaling (e.g. response to auxin, ethylene and brassinosteroid). The category "regulation of transcription" was enriched for genes conserved at DS3, DS4, and DS5. GRs were significantly over-represented in subnetworks starting from DS2, indicating that GRs have highly conserved gene network neighborhoods. Most of the GRs (87%) were conserved in one or more DSs (Figure 2C).

Among the GRs conserved at DS2, 32% were transcription factors (TFs), including regulators of cell cycle (e.g. *AINTEGUMENTA*) and cell elongation such as *BEE2* and its homolog *HBI1* (Supplemental Figure S3). These results suggest a conserved role of these TFs in leaf development across the three plant species. Genes involved in hormone-mediated transcriptional regulation (*INDOLEACETIC ACID-INDUCED PROTEIN (IAA)3, IAA14, IAA30,* and *AUXIN RESISTANT* (*AUX*)*1*) were also detected. Cell growth regulators, including the GRF family, were found conserved and, among them, *GRF2* was conserved at DS2. Literature information on differentially expressed gene (DEG) sets from perturbation experiments was also included in the functional enrichment analyses for several primary-GRs. In particular, genes up- and down-regulated in *SAMBA* loss-of-function mutants (Eloy et al., 2012) and *JAW (JAGGED AND WAVY)* overexpression lines (Gonzalez et al., 2010) were significantly enriched in the GR-related set (Figure 2B). Whereas *SAMBA* plays a key role in organ size control (seeds, leaves and roots), transgenic overexpression lines of *JAW* showed enlarged leaves and an increased cell number, indicative of prolonged cell proliferation (Gonzalez et al., 2010; Eloy et al., 2012). An additional functional enrichment analysis was performed focusing on TF families to identify their cross-species conservation level. In particular, genes conserved from DS2 to DS5 (Supplemental Figure S4) were significantly enriched for the ETHYLENE RESPONSE FACTOR (ERF) family (q-value $< 0.01$), which has a recognized role in plant growth (Dubois et al., 2018). At DS3, among others, MYB and WRKY TF families, known to be involved in developmental processes, appeared strongly conserved. At the least stringent DSs (DS4 and DS5) we could observe other conserved TF families like DOF (regulating the transcriptional machinery in plant cells), MIKC-MADS

(involved in floral development) and NAC (with functions in plant growth, development and stress responses) (Lehti-Shiu et al., 2017). For TFs conserved at DS2, a significant enrichment was observed for the CONSTANS-like TF-family when considering GR-related triplet genes and included *BBX3, BBX4, BBX14* and *BBX16*. A number of BBX proteins have been linked with photomorphogenesis, neighborhood detection, and photoperiodic regulation of flowering (Vaishak et al., 2019).

**Network-based prediction of novel growth regulators**

Apart from analyzing the conservation level of known GRs, we subsequently investigated if new GRs could be identified. To obtain high-quality GR predictions, a combined strategy was adopted to leverage the known GRs and the gene neighborhood conservation analysis through a guilt-by-association (GBA) approach. The GBA principle states that genes with related function tend to be protein interaction partners or share features such as expression patterns or close network neighborhood (Oliver Stephen, 2000). First, gene function prediction through GBA was performed, where the known GRs were used as guide genes for network-based gene function discovery (Figure 1, step 4b). Gene functions were assigned through functional enrichment in the Arabidopsis networks, at different DSs. As a result, genes that were part of network neighborhoods significantly enriched for guide GRs were classified as predicted GRs, and a GBA score was assigned to quantify the strength of the predicted GRs (see Materials and Methods). Secondly, the predictions (Figure 1, step 4b) were filtered for those already identified as triplet genes (Figure 1, step 4a). These filtered predictions (Figure 1, step 5), forming the predicted GR set, were labelled with their species names if they were part of the guide GRs (primary or translated-GR) or with "new" if they were novel (Supplemental Table S3). This approach led to 2206 GR predictions, of which 66 were guide GRs. For the latter, 11 were uniquely from the Arabidopsis GR primary set, 53 uniquely from the aspen translated-GRs, and the remaining two were shared among species. Note that the recovery of known GR genes would be zero in case the network would be random and not capture growth-related transcriptional information. From DS1 to DS5, the subsets of GR predictions covered 175, 496, 421, 891 and 223 genes, respectively (Supplemental Table S3). Overall, the biological processes observed for the conserved predictions agreed with those observed for all triplet genes (Figure 2).

To evaluate the reliability of the predicted GR set and its potential use for discovering genes with a significant effect on plant growth, the public phenotype database RARGE II (Akiyama et al., 2014), covering 17,808 genes and 35,594 lines, was screened obtaining a list of 391 Arabidopsis genes that, if mutated, caused a phenotype change in Arabidopsis leaf length, width and/or size (RARGE II leaf trait genes, Supplemental Table S4). When investigating the gene recovery for the RARGE II leaf trait genes (Figure 3), a clear trend was observed in phenotype recovery ranging from DS1, with higher recovery (~3 and ~4.3 fold enrichment compared to what is expected by chance for proliferation and expansion, respectively), to DS5, with almost no recovery. This result indicates that, among all DSs, DS5 is the least suitable one to identify genes with a potential effect on leaf phenotype.

**Validation of GR predictions using literature and leaf phenotyping**

To validate the assumption that the GR predictions top ranked by GBA are more likely to show a plant growth-related phenotype, an in-depth literature analysis was performed to summarize the connection with different growth-related pathways (Supplemental Table S5) and to score known growth-related phenotypes for the top 100 GR predictions (Supplemental Table S6). For 61 of these 100 predicted genes, mutant lines and/or lines with ectopic expression were reported. For 34 out of the 61 genes (55.7%), obvious alterations to leaf size and shape as well as petiole length were reported when mutated or overexpressed (Supplemental Table S6).

Functional analysis of the 34 genes with described leaf phenotypes revealed their involvement in several biological processes and pathways such as cell cycle regulation, hormone response, photosynthesis, carbon utilization and cell wall modification (Figure 4). Importantly, we could find conserved relationships between five specific genes active in the expansion phase: CATIONIC AMINO ACID TRANSPORTER *(CAT)2*, *THIOREDOXIN* X *(THX)*, BETA CARBONIC ANHYDRASE *(BCA)4*, *CA2*, and *PMDH2*. Among them, *CAT2* and *BCA4* were also high ranked by GBA score. For the proliferation cluster, we could observe strong relationships between *ANT*, *OBF BINDING PROTEIN 1* (*OBP1)*, *GRF2*, *CYCD3;3*, *GLABRA 1* (*GL1)*, *HTA8 (HISTONE H2A 8)*, and *AN3*. Among them, we identified TFs mainly involved in cell cycle process (*ANT*, *OBP1*, *GRF2*), cell wall (*GL1*), and hormone signaling pathways such as jasmonate (*GL1*), abscisic acid (*ANT*), and gibberellin (*GL1*). Twenty-seven of the 61 predictions with knock-down mutations and/or ectopic expression lines did not show a association with leaf growth, which

may be partially due to the redundancy of large gene families or that the leaf phenotype was not explored in those studies. Additionally, three of these 27 genes have been reported to influence root or hypocotyl development, which may also contribute to overall plant growth and organ size.

To further validate the role of these candidate GRs in the leaf development, the system that we chose to study plant growth, we collected the mutants of nine genes among the 27 predicted GRs which have not been reported with a leaf phenotype (Supplemental Table S7). Molecular identification of these mutants was conducted and a detailed analysis of leaf growth in controlled long-day soil-grown conditions was made (Supplemental Figure S5). By following the projected rosette area (PRA), compactness and stockiness of each mutant line over time, this phenotypic characterization revealed that the mutants of two GR candidate genes showed altered rosette growth. The mutant lines of a putative nitrate transporter gene *NPF6.4/NRT1.3*, *sper3-1* and *sper3-3*, both displayed decreased PRA compared with the wild-type plants (Figure 5A). The *sper3-1* harbored a mutation at a conserved glutamate *of NRT1.3*, while the T-DNA line *sper3-3* was a knockout allele (Tong et al., 2016). The reduction in size of *sper3-3* was smaller and occurred later in development compared with *sper3-1*. Before bolting (26 DAS), *sper3-1* and *sper3-3* were 37.3% and 13.2% smaller, respectively, compared with the wild-type (Supplemental Table S7). Both *sper3-1* and *sper3-3* showed significantly reduced leaf number compared to wild type (Figure 5, Supplemental Figure S6). Besides *NPF6.4*, the mutants of *LATE MERISTEM IDENTITY2* (*LMI2*) which has been reported to be required for correct timing of the meristem identity transition (Pastore et al., 2011), also showed altered rosette growth. In standard long-day conditions in soil, a significant reduction of PRA was detected in *lmi2-1*, which displayed elevated *LMI2* expression in seedlings. By contrast, the *lmi2-2* mutants in which the T-DNA insertion gave rise to a truncated non-functional LMI2 protein, exhibited significantly increased PRA and were 13.5% larger than the wild-type plants at 26 DAS (Figure 5B and Supplemental Table S7). Among *LMI2 mutants, lmi2-2* showed significantly increased leaf number (Figure 5, Supplemental Figure S6). Both *NPF6.4* and *LMI2* were highly ranked by GBA (rank 18 and 20, respectively), which further implies that the predictions with a low GBA score are more likely to show a leaf phenotype. Although the leaf was the model system chosen and analyzed in this study, we do not exclude that the predicted candidate GRs, including the validated *NPF6.4* and *LMI2*, might also alter the growth of other organs. Taken together, these experimentally validated genes lend additional support to the potential of our predictions for plant growth regulation.

## Discussion

In this study, we developed an integrative approach to identify candidate genes responsible for altering plant growth. To accomplish this, we used cross-species gene network analysis focusing on the leaf, given its similarities between dicots and monocots (Nelissen et al., 2016). To identify relevant context-specific gene interactions, it is highly recommended to focus the gene network analysis on a specific condition or context, rather than integrating multiple conditions (e.g. different stresses, growth conditions, development stages) (Pavlidis and Gillis, 2012; Liseron-Monfils and Ware, 2015; Serin et al., 2016). For this reason, expression datasets were generated and compiled capturing two main features of leaf growth: cell proliferation and cell expansion. These two processes are governed by similar cellular and molecular pathways across monocots and dicots (Nelissen et al., 2016), which inspired the selection of transcriptional datasets from two dicots (Arabidopsis and aspen) and one monocot (maize). The network construction was carried out integrating multiple inference methods to leverage the power and complementarity of different network inference algorithms (Marbach et al., 2012; Schiffthaler et al., 2018). To evaluate the strength of different biological signals in our network, the gene interactions, obtained after applying different network density cutoffs (DS1-5), were studied. Given that thousands of genes are expressed during leaf development, prioritizing candidate growth regulators starting from different developmental expression datasets is a major challenge. To do so, we relied on two main approaches: the guilt-by-association principle, which is frequently used for gene discovery, and network neighborhood conservation analysis, which detects significantly overlapping network neighborhoods across species to identify reliable functional orthologs (Movahedi et al., 2011; Netotea et al., 2014).

From the gene neighborhood conservation analysis on five different density subnetworks, we observed that, with an increased network density, the number of genes with conserved network neighborhood also grew. This is expected and is probably due to a greater statistical power when comparing larger neighborhoods (Netotea et al., 2014). Overall, as previously observed (Vercruysse et al., 2020b), the integration of different sequence-based orthology detection methods was important because of their complementarity, highlighting complex orthology relationships and evaluating the strength of the orthology support. Overall, 36% of the Arabidopsis genes (7,320 out of 20,313 genes present in the network) had conserved neighborhoods across Arabidopsis, aspen,

and maize, in any of the five density subnetworks. This result is similar to what has been found across Arabidopsis, poplar and rice, although a different network construction pipeline was used there (Netotea et al., 2014).

From a plant breeding perspective, we were interested in cross-species functionally conserved predictions with experimental evidence in more than one species. *GA20-oxidase1* represents a well-known example of a GR that is functionally conserved across monocots and dicots. This gene was confirmed in our analyses to be conserved at the network neighborhood level. *GA20-oxidase1* is in fact a rate limiting enzyme for gibberellin growth hormone biosynthesis in Arabidopsis, aspen, maize and rice (Gonzalez et al., 2010; Nelissen et al., 2012; Qin et al., 2013; Eriksson et al., 2000). To validate the functional relevance of the predicted GRs, we screened the top 100 GR predictions and observed that, among the 34 Arabidopsis predicted genes with a known leaf phenotype in Arabidopsis, six were also already known to affect plant growth in aspen (here stem size). This result is not unexpected as overlapping regulatory mechanisms and genes are shared between primary and secondary meristems, which are responsible for the formation of plant tissues and organs (Baucher et al., 2007). The six translated-GRs were *AUX1*, *IAA3*/*SHY2*, *AUXIN RESISTANT 5 (AXR5)*, *ATBS1 INTERACTING FACTOR 3 (AIF3)*, *AIF4*, and *HOMOLOG OF BEE2 INTERACTING WITH IBH 1 (HBI1)* and their expression in Arabidopsis was peaking at the cell expansion phase. The first three genes are auxin-related genes. Auxin is important for regulating root meristem growth and is crucial for root initiation and lateral root number. *AUX1* was translated from aspen Potra002054g16021 while *IAA3*/*SHY2* and *AXR5* were translated from aspen Potra000605g04596. For both these aspen genes, generated aspen RNAi lines exhibited an increase in stem size, an important indicator for tree biomass yield, connecting back to the underlying regulatory processes in the meristematic tissues (Supplemental Table S2). *AUX1* is an auxin transport protein which regulates auxin distribution across source (young leaf) and sink organs (young roots) (Marchant et al., 2002). *IAA3*/*SHY2* is crucial for root meristem development in Arabidopsis, being the converging point of cytokinin and auxin regulatory circuit (Li et al., 2020). Arabidopsis mutants for *AUX1* and *IAA3*/*SHY2* showed alterations in number and size of lateral roots (Tian and Reed, 1999; Marchant et al., 2002) while *AXR5* is an auxin response factor and mutant plants for this gene are tolerant to auxin and show alterations of root and shoot tropisms (Yang et al., 2004). Our network results and phenotypes in aspen and Arabidopsis indicate that these genes also play an important role in meristem growth in other organs apart from root. *HBI1*,

*AIF3*, and *AIF4*, encode a tier of interacting bHLH transcription factors downstream of BR and regulate the cell elongation in leaf blade and petiole (Bai et al., 2013; Ikeda et al., 2013). *AIF3* and *AIF4* were translated from Potra004144g24626 while *HBI1* was translated from Potra186144g28414. These two aspen genes have been tested with an overexpression approach in aspen trees showing even a bigger increase in stem size as compared with the auxin-related aspen genes Potra000605g04596 and Potra002054g16021 (Supplemental Table S2). Arabidopsis mutants for these genes (*HBI1*, *AIF3*, and *AIF4*) have been linked with alteration of petiole length (Supplemental Table S6).

*LMI2* was a highly ranked GR prediction. Importantly, *LMI2* (a MYB TF) is not a paralog of *LATE MERISTEM IDENTITY 1* (*LMI1*, a homeobox TF), also predicted here. Although *LMI1* and *LMI2* belong to different TF families, they both function downstream of LEAFY to regulate meristem transition (Pastore et al., 2011). *LMI1* was reported to regulate leaf growth in Arabidopsis and other species (Vlad et al., 2014; Andres et al., 2017; Li et al., 2021). Arabidopsis *LMI1* loss-of-function mutant showed decreased leaf serration and promoted tissue growth in stipules (Vuolo et al., 2018). The observed phenotype of mutated *LMI2* was related to an increase of the number of cauline leaves and secondary inflorescences (Pastore et al., 2011). Here, *LMI2* transgenic lines were subjected to phenotypic analysis, which demonstrated that a *LMI2* loss-of-function mutant showed increased leaf number and rosette area. We do not exclude that other organs and/or traits might also be affected by the loss of functionality of this gene. The neighborhood conservation of both *LMI1* and *LMI2* suggests that it would be worthwhile to further explore their roles in leaf shape control across monocots and dicots.

Other known examples of functionally conserved predictions across monocots and dicots were GRFs (e.g. the highly ranked *GRF2*), which have a recognized role in leaf size regulation, and AN3/GIF1, a transcriptional co-activator protein (Nelissen et al., 2016). This was also testified by their network conservation in stringent density subnetworks (DS2). A second gene, *GL1*, had its network neighborhood conserved with GRMZM2G022686 from maize. This maize gene encodes for the MYB-related protein *Myb4*. This protein plays important roles in plant improved tolerance to cold and freezing in Arabidopsis and barley (Soltész et al., 2012), but no connections with growth have been observed for this gene. Arabidopsis *SUC2* showed conservation with GRMZM2G307561, a sucrose/$H^+$ symporter which remobilize sucrose out of the vacuole to the

446 growing tissues. Mutants for this gene showed reduced growth and the accumulation of large
447 quantities of sugar and starch in vegetative tissues in Arabidopsis (Srivastava et al., 2008), while
448 in maize mutants, slower growth, smaller tassels and ears, and fewer kernels were observed (Leach
449 et al., 2017). This gene is thus also important for growth, development, and yield across monocots
450 and dicots.

451 The application of a cross-species approach is an important feature of our methodology. To
452 perform GR predictions, translated-GRs from aspen and maize were also used as guide genes,
453 together with triplets to focus on the conserved parts of the inferred leaf networks. As a result,
454 among the cross-species conserved predictions with experimental evidence in more than one
455 species described above, *AUX1*, *IAA3*/*SHY2*, *AXR5*, *AIF3*, *AIF4*, *HBI1*, *AN3/GIF1*, *GL1*, and
456 *SUC2* couldn't have been predicted using solely primary-GRs from Arabidopsis. This observation
457 indicates that the integration of information of different plant species enhances the detection of
458 GRs.

459 A total of 11 primary-GRs from Arabidopsis showed no network neighborhood conservation. Lack
460 of conservation might be the result of (1) missing orthologs in a target species or (2) different
461 network gene neighbors across species, which in turn might be caused by different transcriptional
462 control. One clear example of no conservation due to a lack of orthologs is PEAPOD 2 (*PPD2)*,
463 which is a TIFY transcriptional regulator part of the PEAPOD (PPD) pathway. This pathway plays
464 an important role in cell proliferation and, with its PPD/KIX/SAP module, is involved in leaf,
465 flower, fruit, and seed development. This pathway is present in most vascular plant lineages, but
466 was lost in monocot grasses (Schneider et al., 2021). The reason for this absence might be found
467 back in intrinsic differences between eudicots and grasses, being mainly lack of meristemoids and
468 functional redundancy for the regulation of cell proliferation. Surprisingly, several non-grass
469 monocot species such as banana (*Musa acuminata)* and oil palm (*Elaeis guineensis)*, the
470 angiosperm *Amborella trichopoda* and lycophytes, carry PPD/KIX/SAP orthologs, although
471 information about their functionality is missing (Schneider et al., 2021). Another gene with
472 orthologs but lacking network neighborhood conservation was *AHK3*, a cytokinin receptor that
473 controls cytokinin-mediated leaf longevity. This might be explained by knock-out experiments on
474 *AHK* receptors showing contrasting effects on flowering time or floral development across
475 Arabidopsis and rice (Burr et al., 2020). Another non-conserved GR was *ZHD5* that regulates

floral architecture and leaf development and is regulated by *MIF1 (MINI ZINC-FINGER 1)* (Hong et al., 2011), which also lacked network conservation. *ZHD5* regulation might thus be different across species. Similarly, FBX*92 (F-BOX PROTEIN92)* was not conserved, which might be explained by the opposite effects on leaf size shown by *ZmFBX92* and *AtFBX92* gain of function in Arabidopsis due to the presence of an F-box-associated domain in *AtFBX92*, lacking in *ZmFBX92*. *FBX92* orthologs might thus undergo different transcriptional regulation (Baute et al., 2017). *EPF1 (EPIDERMAL PATTERNING FACTOR 1)* was also a non-conserved GR. This gene affects stomatal density and water use efficiency. Recent work suggested that, in monocots and dicots, *EPF1* orthologs probably have different temporal dynamics of gene expression in the stomatal lineage (Buckley et al., 2020), which might result in different network gene neighbors.

Based on the validation results of our GR prediction pipeline, a correlation between network size and recovery of genes affecting leaf size was observed. In particular, with increasing network size, the recovery rate decreased, indicating that DS5 is not a recommended network density to use to find growth regulators. The network neighborhood conservation of genes in the most stringent networks involved different basal biological processes, suggesting their functional similarity across monocots and dicots. Not surprisingly, genes involved in cell cycle regulation and plant hormonal response were found, as both processes have a key role in leaf development. Several cell cycle regulators were predicted as GRs, like the cyclin gene *CYCD3;3*, the *CDK* inhibitor *KRP3 (KIP-RELATED PROTEIN)*, and a DOF transcription factor gene *OBP1* (*OBF BINDING PROTEIN 1*) that controls cell cycle progression (Dewitte et al., 2007; Skirycz et al., 2008; Jun et al., 2013). The auxin-responsive transcription factor gene MONOPTEROS (*MP*) is crucial for leaf vascular development (Hardtke and Berleth, 1998), while the Aux/IAA gene that represses auxin signaling, *AXR2*, whose gain-of-function leads to strong inhibition of leaf growth (Mai et al., 2011), was also predicted. Besides auxin, brassinosteroid (BR) and gibberellin (GA) coordinately play key roles in regulating plant cell elongation. The other two predicted transcription factor genes, *HB25* (*HOMEOBOX PROTEIN 25*) and *MYR1*, which modulate bioactive GA biosynthesis, were also shown to have an effect on the petiole growth (Bueso et al., 2014). It is noteworthy that nearly half of all the 34 genes with leaf phenotype were transcription regulators, which highlights the importance of TF-mediated gene expression regulation during leaf development. In addition to hormone-related genes and TFs, genes related to photosynthesis are also important for leaf

development. A carotenoid biosynthesis gene *LCY* and a chloroplast redox-regulating gene *THIOREDOXIN X* were predicted as GR and have been shown to affect leaf size (Li et al., 2009; Pulido et al., 2010). Moreover, the cytoplasmic carbonic anhydrase genes *CA2* and *BCA4* were identified, consistent with the view that carbon utilization in leaves is closely linked to leaf area (DiMario et al., 2016). Cell wall modification is considered to be another important determinant of leaf development. The predicted candidate genes *LACCASE11 (LAC11)* and *CUTICLE DESTRUCTING FACTOR 1* (*CDEF1)*, encoding for a laccase that associates with the lignin deposition in cell wall and a cutinase essential for the degradation of cell wall components, respectively, are also involved in regulating leaf growth and morphology (Takahashi et al., 2010; Qin et al., 2013). Among Arabidopsis genes with a reported phenotype in the RARGE II loss-of-function dataset, *ACO2 (ACC OXIDASE 2)* led to increased leaf size, and AT3G43270, a member of Plant invertase/pectin methylesterase inhibitor superfamily, to smaller leaves. GRs translated from aspen led, through our integrative network approach, to the prediction of *NITRATE TRANSPORTER 1.3* (*NPF6.4*/*NRT1.3)* as a potential GR. In Arabidopsis shoot, the expression of *AtNPF6.4*/*NRT1.3* was induced by nitrate (Okamoto et al., 2003) while, in *Medicago truncatula*, MtNRT1.3 shares 70% identity with *AtNPF6.4*/*NRT1.3* and was reported to be a dual-affinity nitrate transporter (Morre-Le Paven et al., 2011). It was also hypothesized that *NPF6.4*/*NRT1.3* may play a role in supplying nitrate to photosynthesizing cells (Tong et al., 2016). In our experiments, we showed that this gene, when mutated, is altering leaf growth. This cross-species conserved gene would thus contribute to nitrogen assimilation, that, closely interacting with carbon metabolism, sustains plant growth and development (Nunes-Nesi et al., 2010). Due to the relevance and the strong interconnection of the processes where *NPF6.4/NRT1.3* and many of the candidate GRs here predicted, are involved in, future experimental work will have to reveal the role of these candidate GRs in other organs.

In conclusion, the approach developed in this study fully exploits the potential of integrative biology to translate and expand yield-related functional annotations in different plant species, as such accelerating crop breeding.

## Materials and Methods

### Integration of developmental expression datasets and network construction

Transcriptomic datasets were obtained from a list of studies in Arabidopsis, maize and aspen covering samples from the main leaf developmental phases (Supplemental Table S1, Supplemental Methods, Supplemental Dataset S1). Details about these datasets and the processing of these samples were reported in Supplemental Methods. Maize data was mainly composed by a developmental compendium generated in this work (Supplemental Methods). The network inference was carried out with Seidr (Schiffthaler et al., 2018), which infers gene networks by using multiple inference algorithms and then aggregating them into a meta-network. This approach has been shown to strongly improve the accuracy of the results (Marbach et al., 2012). Each network was subset into five density subnetworks (DSs) using five different network density values. This procedure consisted in selecting the top 0.1, 0.5, 1, 5 and 10% top Seidr links in each species-specific network and generating five DSs (from the most stringent DS1 to the least stringent DS5).

### Orthology and network neighborhood conservation

To compute cross-species gene network neighborhood conservation, orthology information between genes from Arabidopsis, maize and aspen was computed using the PLAZA comparative genomics platform (Van Bel et al., 2018). A custom version of this platform was built covering in total 15 eukaryotic species including *Arabidopsis thaliana* (TAIR10), *Eucalyptus grandis* (v2.0), *Populus trichocarpa* (v3.01), *Populus tremula* (v1.1), *Vitis vinifera* (12X March 2010 release), *Zea mays* (AGPv3.0), *Oryza sativa* ssp. *Japonica* (MSU RGAP 7), *Triticum aestivum* (TGACv1), *Amborella trichopoda* (Amborella v1.0), *Picea abies* (v1.0), *Pinus taeda* (v1.01), *Selaginella moellendorffii* (v1.0), *Physcomitrium patens* (v3.3), *Chlamydomonas reinhardtii* (v5.5) and *Micromonas commode* (v3.0). PLAZA allows identifying orthologs using different methods (evidences), corresponding to orthologous gene families inferred through sequence-based clustering with OrthoFinder (Emms and Kelly, 2015), phylogenetic trees, and multispecies Best-Hits-and-Inparalogs families (Van Bel et al., 2012). The PLAZA orthology relationships were extracted and filtered retaining all orthologs having a requirement of 2/3 orthology evidences and, for those with 1/3 evidence and >25 orthologs, the ones corresponding to the best 25 blast hits

(sorted by e-value) were retained. The generated orthology output was used for the following pipeline steps.

The generated DSs and the orthology information were used to compare the three species using a network neighborhood conservation analysis (ComPlEx analysis, as in Netotea et al. 2014). In this analysis, the network neighborhood of a gene (i.e. all genes with a link to it) was considered conserved if it had a statistically significant ($q < 0.05$) overlap with the network neighborhood of its ortholog in the other species (Netotea et al., 2014). Here, the comparison was performed for all pairs of networks between the datasets of the three species, and the output of this analysis was collated to create "triplets". The triplets are sets of three orthologous genes–one per network/species–that have a significantly conserved network neighborhood in all three pairs of comparisons. Since the test is not commutative, the neighborhoods had to be significantly conserved in both directions of the test. To estimate the false discovery rate (FDR) of the detection of triplets, a permutation strategy was adopted. For 500 runs of ComPlEx, ortholog relationships were shuffled, keeping the relative number of orthologs per gene and per species, and then comparing the number of triplets computed from randomization with those resulting using the original (unshuffled) orthologs.

**Functional analyses and prediction of growth regulators**

Gene Ontology (Ashburner et al., 2000) functional annotations for Arabidopsis, maize and aspen were retrieved from TAIR (download 25/12/2018), Gramene (AGPv3.30, http://bioinfo.cau.edu.cn/agriGO/download.php), and PlantGenIE (ftp://ftp.plantgenie.org/Data/PopGenIE/Populus_tremula/v1.1/annotation/), respectively, and filtered for the genes present in the corresponding species networks. We focused on biological processes (BP) and excluded the general GO BP terms with >= 1500 genes as well as GO terms with <= 10 genes to avoid biases towards very general and specific terms. For each gene, all GO annotations were recursively propagated in order to include parental GO terms. Functional over-representation analyses were performed using the hypergeometric distribution together with Benjamini-Hochberg (BH) correction for multiple testing (Benjamini and Hochberg, 1995). To get a complete view on all relevant processes related to plant growth, information from literature was collected on growth regulators (GRs). Experimentally validated genes in Arabidopsis, maize and aspen (primary-GRs) were retrieved from public databases (Gonzalez et al., 2010; Beltramino et

al., 2018). Experimentally validated aspen genes were obtained by access to SweTree Technologies private database that contains data from the large-scale testing of >1,000 genes and their growth-related properties (here only "stem size" was taken into consideration), an effort where more than 1,500 recombinant DNA constructs were used to either introduce a gene product or alter the level of an existing gene product by over-expression or RNA interference in aspen trees, whose growth characteristics were then monitored in greenhouse and field experiments to provide extensive gene-to-yield data. The Arabidopsis GR primary set was then enlarged with high quality GR orthologs from maize and aspen using the triplets ("translated-GRs") to obtain a combined GR set. The combined set was finally filtered with genefilter package from Bioconductor (Gentleman et al., 2021) to remove genes with small expression variance (var.func=IQR, var.cutoff=0.8) and focus on genes active during proliferation or expansion phases of leaf development ("expression-supported GRs", Supplemental Table S2). Other information on functional categories (Vercruysse et al., 2020a) and differentially expressed genes from relevant studies on plant development was also included in the functional enrichment analyses (Anastasiou et al., 2007; Gonzalez et al., 2010; Eloy et al., 2012; Vercruyssen et al., 2014).

The expression-supported GRs were used as guide genes to perform network-guided gene function prediction via a guilt-by-association (GBA) approach. This approach is based on the assumption that genes close to the input GRs in the network are likely to have similar functions. The GBA approach was applied to attribute functions based on GO enrichment in the modules of each DS yielding five sets of gene predictions. By this procedure, gene neighborhoods significantly enriched for guide GRs were functionally annotated (hypergeometric distribution). This allowed to predict candidate GRs and estimate, for each of them, a corresponding FDR adjusted p-value (or q-value), which was renamed "GBA-score". The GBA score is a confidence score that ranks genes high if they are connected with many GRs in the network (in fact high ranked genes have a low GBA score as this is an indicator of a strong enrichment). For an example GR prediction (in one of any of the five DSs), the GBA-score from the five DSs was summarized taking the mean of the GBA-scores and setting the GBA-score to 0.05 for the DSs where the gene was not predicted. This yielded a list of GR predictions that was then further filtered by only retaining those predictions having conserved neighborhood in at least one DS. To perform a validation of the gene function predictions, the RARGE II (Akiyama et al., 2014) database was interrogated to retrieve a list of Arabidopsis genes that, when mutated, showed an increased or decreased length,

width and size for rosette leaf, vascular leaf and cauline leaf (leaf trait genes). This gene set was used to analyze the recovery at each DS of leaf growth-related phenotypes. For the top 100 predictions ranked by GBA-score a manual literature search was performed to retrieve all genes with a reported phenotype including information about the biological pathway the gene might be active in, and other public functional annotations.

**Rosette growth phenotyping**

The *Arabidopsis thaliana* ecotype Columbia-0 (Col-0) was used as the wild-type in this study. The T-DNA insertion lines for At4g26530 (Salk_080758/*fba5-1*), At3g21670 (Salk_001553/*sper3-3*), At3g61250 (Salk_066767/*lmi2-1*, Salk_020792/*lmi2-2*), At4g25240 (Salk_113731), At1g63470 (Salk_123590/*ahl5*), At4g37980 (Salk_001773/*chr hpl*), At2g38530 (Salk_026257/*ltp2-1*), At4g28950 (Salk_019272), and At1g12240 (Salk_016136) were confirmed using PCR with a T-DNA primer and gene-specific primers (Supplemental Table S8) (Lu et al., 2012; Zhao et al., 2013; Jacq et al., 2017; Tanaka et al., 2018; Pastore et al., 2011; Tong et al., 2016). All tested seeds were stratified in the darkness at 4 °C for 3 days and then sown on soil in the 7 cm wide square pots with a density of four seeds per pot. After 8 days in the growth room (with controlled temperature at 22 °C and light intensity 110 μmol $m^{-2}$ $s^{-1}$ in a 16 h/8 h cycle), the four seedlings were screened, leaving one seedling per pot, which most closely resembled the genotype average. The plants were imaged in a phenotyping platform (MIRGIS) with fixed cameras located directly above the plants, which images plants at the same time every day. These images were then processed to extract the rosette growth parameters of each plant. The mean PRA, compactness and stockiness values were calculated over time for each genotype.

**Accession Numbers**

Sequence data from this article have been submitted to ENA (E-MTAB-11108). NPF6.4/NRT1.3 and LATE MERISTEM IDENTITY2 have locus identifier AT3G21670 and AT3G61250, respectively.

**Supplemental data**

Supplemental Figure S1. Number of neighbors per gene at each density subnetwork in Arabidopsis.

Supplemental Figure S2. Expression patterns for the expression-supported growth regulators in Arabidopsis.

Supplemental Figure S3. Expression-supported growth regulators with neighborhood conservation at each network density level.

Supplemental Figure S4. Functional enrichment of cross-species conserved transcription factors (TF) grouped by TF family.

Supplemental Figure S5. Identification of T-DNA insertion lines.

Supplemental Figure S6. The rosette leaf numbers of the wild-type Col-0 and the mutants of *NRT1.3* and *LMI2*.

Supplemental Table S1. Overview of the expression datasets used for the network computation.

Supplemental Table S2. List of expression-supported growth regulators.

Supplemental Table S3. Predicted growth regulators.

Supplemental Table S4. List of RARGE II leaf trait genes known to affect leaf phenotype if mutated.

Supplemental Table S5. Top 100 predicted growth regulators annotated.

Supplemental Table S6. In depth literature analysis for the top 100 predicted growth regulators.

Supplemental Table S7. List of genes tested for leaf phenotype in this study.

Supplemental Table S8. Primers used for T-DNA identification and qPCR.

Supplemental Dataset S1. Expression datasets for Arabidopsis, maize, and aspen.

Supplemental Dataset S2. Triplets generated with ComPlEx.

Supplemental Methods. Detailed methods for expression dataset retrieval, generation, and processing.

**Funding information:** TRH, KV and NRS was partially funded by the Research Council of Norway (project number 287465).

677 **Acknowledgements**

678 We thank Taku Takahashi (Okayama University, Japan) for kindly sending us the *sper3-*
679 *1* and *sper3-3* seeds, and Julie Pevernagie for her technical support.

## Figure legends

**Figure 1**. **Outline of the cross-species network approach to identify candidate growth regulators**. For Arabidopsis, maize and aspen, the expression data (step 1) is used as input to construct a fully connected meta-network per species (step 2). Subsequently, each meta-network is split into five density subnetworks (DSs) by applying specific density cutoffs (step 3). These DSs are the input for two different analyses: they are used first as input to compute cross-species gene neighborhood conservation (step 4a). Secondly, they are used to predict functions via guilt-by-association (step 4b). This leads to gene function annotations of query genes (blue circles) based on prior knowledge on growth regulators (purple circles). Edge thickness defines in which subnetwork the interaction is conserved (line thickness represents the DS and ranges from 1, the most stringent DS represented by the thickest line, to 5, the least stringent DS represented by the thinnest line). Finally, the results of these two analyses (steps 4a and 4b) are integrated to obtain a list of candidate growth regulators (step 5).

**Figure 2**. **Triplets and their functional enrichments in cross-species conserved leaf networks.** (A) The number of triplet genes showing cross-species gene neighborhood conservation is plotted for all density subnetworks (DSs). (B) The biological process functional over-representation at each DS is summarized for two sets: (1) all triplet genes (All) and (2) growth regulators and their network neighbor (Growth regulator-related) triplet genes, subset of all triplet genes. Functional categories marked with asterisks (*) belong to leaf growth modules described in Vercruysse et al. (2020) and to the differentially expressed gene sets from relevant studies on plant development (Bezhani et al., 2007; Gonzalez et al., 2010; Eloy et al., 2012; Vercruyssen et al., 2014; Vanhaeren et al., 2017). For clarity, long biological process names have been abbreviated ([§]). (C) Overview of growth regulators with (and without) cross-species neighborhood conservation at different DSs.

**Figure 3. Recovery of RARGE II leaf trait genes for each density subnetwork split in proliferation and expansion**. The grey dashed line indicates the leaf-related phenotype gene recovery expected by chance (within the RARGE II dataset).

**Figure 4**. **Gene-function network of the 34 phenotype-related genes out of the top 100 predicted growth regulators**. Predictions are clustered by expression profile (proliferation on the left and expansion on the right). Node label colours from dark green (weak) to yellow (strong) represent the reliability of the gene prediction (GBA score). Node border colours indicate known growth regulators from Arabidopsis (black), known growth regulators from aspen (red), and Arabidopsis known growth regulator paralogs (violet). Diamonds represent transcription factors. Links from dark orange thick (DS1) to light orange thin (DS5) represent the density subnetwork where the genes were found connected. Genes are linked with their respective growth-related pathways (centered if connecting to both proliferation and expansion related genes) by grey links. Anti-correlation links (connecting proliferation with expansion genes) were removed for clarity.

**Figure 5**. **Mutants of predicted growth regulators *NRT1.3* and *LMI2* showed altered rosette growth**. (A-B) Dynamic growth analysis of projected rosette area, compactness and stockiness over time of wild-type Col-0 and the mutants of *NRT1.3* (A) and *LMI2* (B) in soil. Values are means ± SD. For phenotypic analysis of mutants of *LMI2*, sample sizes (n) were n=16 for Col-0, n=16 for *lmi2-2*, and n=17 for *lmi2-1*. For phenotypic analysis of mutants of *NRT1.3*, n=14 for Col-0, n=15 for *sper3-1*, and n=13 for *sper3-3*. The asterisks represent the time points at which differences in the PRA become significant between the mutants and wild-type, as determined by Student's t test (*, $P<0.05$; **, $P<0.01$). The experiments were repeated three times with similar results, and one representative experiment is shown. (C-D) Phenotype of 26-day-old mutants of *NRT1.3* (C) and *LMI2* (D). Scale bar = 1 cm.

## References


Akiyama K, Kurotani A, Iida K, Kuromori T, Shinozaki K, Sakurai T (2014) RARGE II: An integrated phenotype database of arabidopsis mutant traits using a controlled vocabulary. Plant Cell Physiol 55: 1–10

Anastasiou E, Kenz S, Gerstung M, MacLean D, Timmer J, Fleck C, Lenhard M (2007) Control of Plant Organ Size by KLUH/CYP78A5-Dependent Intercellular Signaling. Dev Cell 13: 843–856

Andres RJ, Coneva V, Frank MH, Tuttle JR, Samayoa LF, Han SW, Kaur B, Zhu L, Fang H,

734 Bowman DT, et al (2017) Modifications to a LATE MERISTEM IDENTITY gene are
735 responsible for the major leaf shapes of Upland cotton (Gossypium hirsutum L.). Proc Natl
736 Acad Sci U S A 114: E57–E66

737 Ashburner M, Ball CA, Blake JA, Botstein D, Butler H, Cherry JM, Davis AP, Dolinski K, Dwight
738 SS, Eppig JT, et al (2000) Gene ontology: Tool for the unification of biology. Nat Genet 25:
739 25–29

740 Bai MY, Fan M, Oh E, Wang ZY (2013) A triple helix-loop-helix/basic helix-loop-helix cascade
741 controls cell elongation downstream of multiple hormonal and environmental signaling
742 pathways in Arabidopsis. Plant Cell 24: 4917–4929

743 Barboza L, Effgen S, Alonso-blanco C, Kooke R, Keurentjes JJB, Koornneef M (2013)
744 Arabidopsis semidwarfs evolved from independent mutations in GA20ox1 , ortholog to green
745 revolution dwarf alleles in rice and barley. 110: 15818–15823

746 Baucher M, Jaziri M El, Vandeputte O (2007) From primary to secondary growth : origin and
747 development of the vascular system. 58: 3485–3501

748 Baute J, Polyn S, De Block J, Blomme J, Van Lijsebettens M, Inzé D (2017) F-box protein FBX92
749 affects leaf size in Arabidopsis thaliana. Plant Cell Physiol 58: 962–975

750 Baxter I (2020) We aren’t good at picking candidate genes, and it’s slowing us down. Curr Opin
751 Plant Biol 54: 57–60

752 Beltramino M, Ercoli MF, Debernardi JM, Goldy C, Rojas AML, Nota F, Alvarez ME,
753 Vercruyssen L, Inzé D, Palatnik JF, et al (2018) Robust increase of leaf size by Arabidopsis
754 thaliana GRF3-like transcription factors under different growth conditions. Sci Rep 8: 1–13

755 Benjamini Y, Hochberg Y (1995) Controlling the False Discovery Rate: A Practical and Powerful
756 Approach to Multiple Testing. J R Stat Soc Ser B 57: 289–300

Bezhani S, Winter C, Hershman S, Wagner JD, Kennedy JF, Chang SK, Pfluger J, Su Y, Wagner D (2007) Unique, shared, and redundant roles for the Arabidopsis SWI/SNF chromatin remodeling ATPases Brahma and Splayed. Plant Cell 19: 403–416

Buckley CR, Caine RS, Gray JE (2020) Pores for Thought: Can Genetic Manipulation of Stomatal Density Protect Future Rice Yields? Front Plant Sci 10: 1783

Bueso E, Muñoz-Bertomeu J, Campos F, Brunaud V, Martínez L, Sayas E, Ballester P, Yenush L, Serrano R (2014) ARABIDOPSIS THALIANA HOMEOBOX25 uncovers a role for gibberellins in seed longevity. Plant Physiol 164: 999–1010

Burr CA, Sun J, Yamburenko M V., Willoughby A, Hodgens C, Boeshore SL, Elmore A, Atkinson J, Nimchuk ZL, Bishopp A, et al (2020) The HK5 and HK6 cytokinin receptors mediate diverse developmental pathways in rice. Development. 147:dev191734

Cheng CY, Li Y, Varala K, Bubert J, Huang J, Kim GJ, Halim J, Arp J, Shih HJS, Levinson G, et al (2021) Evolutionarily informed machine learning enhances the power of predictive gene-to-phenotype relationships. Nat Commun 12: 1–15

De Smet R, Marchal K (2010) Advantages and limitations of current network inference methods. Nat Rev Microbiol 8: 717–729

Dewitte W, Scofield S, Alcasabas AA, Maughan SC, Menges M, Braun N, Collins C, Nieuwland J, Prinsen E, Sundaresan V, et al (2007) Arabidopsis CYCD3 D-type cyclins link cell proliferation and endocycles and are rate-limiting for cytokinin responses. Proc Natl Acad Sci U S A 104: 14537–14542

DiMario RJ, Quebedeaux JC, Longstreth DJ, Dassanayake M, Hartman MM, Moroney J V. (2016) The cytoplasmic carbonic anhydrases βCA2 and βCA4 are required for optimal plant growth at low CO2. Plant Physiol 171: 280–293

Dubois M, Van den Broeck L, Inzé D (2018) The Pivotal Role of Ethylene in Plant Growth. Trends

781 Plant Sci 23: 311–323

782 Eloy NB, Gonzalez N, Van Leene J, Maleux K, Vanhaeren H, De Milde L, Dhondt S, Vercruysse
783 L, Witters E, Mercier R, et al (2012) SAMBA, a plant-specific anaphase-promoting
784 complex/cyclosome regulator is involved in early development and A-type cyclin
785 stabilization. Proc Natl Acad Sci U S A 109: 13853–13858

786 Emms DM, Kelly S (2015) OrthoFinder: solving fundamental biases in whole genome
787 comparisons dramatically improves orthogroup inference accuracy. 16: 157

788 Eriksson ME, Israelsson M, Olsson O, Moritz T (2000) Increased gibberellin biosynthesis in
789 transgenic trees promotes growth, biomass production and xylem fiber length. Nat Biotechnol
790 18: 784–788

791 Ficklin SP, Feltus FA (2011) Gene coexpression network alignment and conservation of gene
792 modules between two grass species: Maize and rice. Plant Physiol 156: 1244–1256

793 Friedrichsen DM, Nemhauser J, Muramitsu T, Maloof JN, Alonso J, Ecker JR, Furuya M, Chory
794 J (2002) Three redundant brassinosteroid early response genes encode putative bHLH
795 transcription factors required for normal growth. Genetics 162: 1445–1456

796 Gentleman R, Carey VJ, Huber W, Hahne F (2022). genefilter: genefilter: methods for filtering
797 genes from high-throughput experiments. R package version 1.78.0.

798 Gong P, Demuynck K, De Block J, Aesaert S, Coussens G, Pauwels L, Inzé D, Nelissen H (2022)
799 Modulation of the DA1 pathway in maize shows that translatability of information from
800 Arabidopsis to crops is complex. Plant Sci. 321:111295

801 Gonzalez N, de Bodt S, Sulpice R, Jikumaru Y, Chae E, Dhondt S, van Daele T, de Milde L,
802 Weigel D, Kamiya Y, et al (2010) Increased leaf size: Different means to an end. Plant Physiol
803 153: 1261–1279

804 Gray SB, Brady SM (2016) Plant developmental responses to climate change. Dev Biol 419: 64–
805 77

806 Hardtke CS, Berleth T (1998) The Arabidopsis gene MONOPTEROS encodes a transcription
807 factor mediating embryo axis formation and vascular development. EMBO J 17: 1405–1411

808 Heyndrickx KS, Vandepoele K (2012) Systematic identification of functional plant modules
809 through the integration of complementary data sources. Plant Physiol 159: 884–901

810 Hong SY, Kim OK, Kim SG, Yang MS, Park CM (2011) Nuclear import and DNA binding of the
811 ZHD5 transcription factor is modulated by a competitive peptide inhibitor in Arabidopsis. J
812 Biol Chem 286: 1659–1668

813 Inze D, Nelissen H (2022) The translatability of genetic networks from model to crop species:
814 lessons from the past and perspectives for the future. New Phytol

815 Ikeda M, Mitsuda N, Ohme-Takagi M (2013) ATBS1 Interacting Factors negatively regulate
816 Arabidopsis cell elongation in the triantagonistic bHLH system. Plant Signal Behav.
817 8:e23448

818 Jacq A, Pernot C, Martinez Y, Domergue F, Payré B, Jamet E, Burlat V, Pacquit VB (2017) The
819 Arabidopsis lipid transfer protein 2 (AtLTP2) is involved in cuticle-cell wall interface
820 integrity and in etiolated hypocotyl permeability. Front Plant Sci 8: 1–17

821 Jones DM, Vandepoele K (2020) Identification and evolution of gene regulatory networks: insights
822 from comparative studies in plants. Curr Opin Plant Biol 54: 42–48

823 Jun SE, Okushima Y, Nam J, Umeda M, Kim GT (2013) Kip-related protein 3 is required for
824 control of endoreduplication in the shoot apical meristem and leaves of Arabidopsis. Mol
825 Cells 35: 47–53

826 Klie S, Mutwil M, Persson S, Nikoloski Z (2012) Inferring gene functions through dissection of

827 relevance networks: Interleaving the intra- and inter-species views. Mol Biosyst 8: 2233–
828 2241

829 Leach KA, Tran TM, Slewinski TL, Meeley RB, Braun DM (2017) Sucrose transporter2
830 contributes to maize growth, development, and crop yield. J Integr Plant Biol 59: 390–408

831 Lee BH, Ko JH, Lee S, Lee Y, Pak JH, Kim JH (2009) The Arabidopsis GRF-Interacting Factor
832 gene family performs an overlapping function in determining organ size as well as multiple.
833 Plant Physiol 151: 655–668

834 Lee I, Ambaru B, Thakkar P, Marcotte EM, Rhee SY (2010) Rational association of genes with
835 traits using a genome-scale gene network for Arabidopsis thaliana. Nat Biotechnol 28: 149–
836 156

837 Lee T, Lee S, Yang S, Lee I (2019) MaizeNet: a co-functional network for network-assisted
838 systems genetics in Zea mays. Plant J 99: 571–582

839 Lee T, Yang S, Kim E, Ko Y, Hwang S, Shin J, Shim JE, Shim H, Kim H, Kim C, et al (2015)
840 AraNet v2: An improved database of co-functional gene networks for the study of
841 Arabidopsis thaliana and 27 other nonmodel plant species. Nucleic Acids Res 43: D996–
842 D1002

843 Lehti-Shiu MD, Panchy N, Wang P, Uygun S, Shiu SH (2017) Diversity, expansion, and
844 evolutionary novelty of plant DNA-binding transcription factor families. Biochim Biophys
845 Acta - Gene Regul Mech 1860: 3–20

846 Li J, Yuan D, Wang P, Wang Q, Sun M, Liu Z, Si H, Xu Z, Ma Y, Zhang B, et al (2021) Cotton
847 pan-genome retrieves the lost sequences and genes during domestication and selection.
848 Genome Biol 22: 1–26

849 Li T, Kang X, Lei W, Yao X, Zou L, Zhang D, Lin H (2020) SHY2 as a node in the regulation of
850 root meristem development by auxin, brassinosteroids, and cytokinin. J Integr Plant Biol 62:

1500–1517

Li Z, Ahn TK, Avenson TJ, Ballottari M, Cruz JA, Kramer DM, Bassi R, Fleming GR, Keasling JD, Niyogi KK (2009) Lutein accumulation in the absence of zeaxanthin restores nonphotochemical quenching in the arabidopsis thaliana npq1 mutant. Plant Cell 21: 1798–1812

Liseron-Monfils C, Ware D (2015) Revealing gene regulation and associations through biological networks. Curr Plant Biol 3–4: 30–39

Lu W, Tang X, Huo Y, Xu R, Qi S, Huang J, Zheng C, Wu C ai (2012) Identification and characterization of fructose 1,6-bisphosphate aldolase genes in Arabidopsis reveal a gene family with diverse responses to abiotic stresses. Gene 503: 65–74

Mai YX, Wang L, Yang HQ (2011) A Gain-of-Function Mutation in IAA7/AXR2 Confers Late Flowering under Short-day Light in Arabidopsis. J Integr Plant Biol 53: 480–492

Marbach D, Costello JC, Küffner R, Vega NM, Prill RJ, Camacho DM, Allison KR, Kellis M, Collins JJ, Aderhold A, et al (2012) Wisdom of crowds for robust gene network inference. Nat Methods 9: 796–804

Marchant A, Bhalerao R, Casimiro I, Eklöf J, Casero PJ, Bennett M, Sandberg G (2002) AUX1 promotes lateral root formation by facilitating indole-3-acetic acid distribution between sink and source tissues in the Arabidopsis seedling. Plant Cell 14: 589–597

Mizukami Y, Fischer RL (2000) Plant organ size control: AINTEGUMENTA regulates growth and cell numbers during organogenesis. Proc Natl Acad Sci U S A 97: 942–947

Morre-Le Paven MC, Viau L, Hamon A, Vandecasteele C, Pellizzaro A, Bourdin C, Laffont C, Lapied B, Lepetit M, Frugier F, et al (2011) Characterization of a dual-affinity nitrate transporter MtNRT1.3 in the model legume Medicago truncatula. J Exp Bot 62: 5595–5605

874 Movahedi S, van De Peer Y, Vandepoele K (2011) Comparative network analysis reveals that
875 tissue specificity and gene function are important factors influencing the mode of expression
876 evolution in arabidopsis and rice. Plant Physiol 156: 1316–1330

877 Movahedi S, Van Bel M, Heyndrickx KS, Vandepoele K (2012) Comparative co-expression
878 analysis in plant biology. Plant, Cell Environ 35: 1787–1798

879 Mutwil M, Klie S, Tohge T, Giorgi FMM, Wilkins O, Campbell MMM, Fernie ARR, Usadel B,
880 Nikoloski Z, Persson S (2011) PlaNet: Combined Sequence and Expression Comparisons
881 across Plant Networks Derived from Seven Species. Plant Cell 23: 895–910

882 Nelissen H, Gonzalez N, Inzé D (2016) Leaf growth in dicots and monocots: So different yet so
883 alike. Curr Opin Plant Biol 33: 72–76

884 Nelissen H, Rymen B, Jikumaru Y, Demuynck K, Van Lijsebettens M, Kamiya Y, Inzé D,
885 Beemster GTS (2012) A local maximum in gibberellin levels regulates maize leaf growth by
886 spatial control of cell division. Curr Biol 22: 1183–1187

887 Netotea S, Sundell D, Street NR, Hvidsten TR (2014) ComPlEx: Conservation and divergence of
888 co-expression networks in A. thaliana, Populus and O. sativa. BMC Genomics 15: 106

889 Nowicka B (2019) Target genes for plant productivity improvement. J Biotechnol 298: 21–34

890 Nuccio ML, Paul M, Bate NJ, Cohn J, Cutler SR (2018) Where are the drought tolerant crops? An
891 assessment of more than two decades of plant biotechnology effort in crop improvement.
892 Plant Sci 273: 110–119

893 Nunes-Nesi A, Fernie AR, Stitt M (2010) Metabolic and signaling aspects underpinning the
894 regulation of plant carbon nitrogen interactions. Mol Plant 3: 973–996

895 Obertello M, Shrivastava S, Katari MS, Coruzzi GM (2015) Cross-species network analysis
896 uncovers conserved nitrogen-regulated network modules in rice. Plant Physiol 168: 1830–

1843

Oliver Stephen (2000) Guilt-by-association goes global. Nature 403: 601–603

Okamoto M, Vidmar JJ, Glass ADM (2003) Regulation of NRT1 and NRT2 gene families of Arabidopsis thaliana: Responses to nitrate provision. Plant Cell Physiol 44: 304–317

Pastore JJ, Limpuangthip A, Yamaguchi N, Wu M-F, Sang Y, Han S-K, Malaspina L, Chavdaroff N, Yamaguchi A, Wagner D (2011) LATE MERISTEM IDENTITY2 acts together with LEAFY to activate APETALA1. Development 138: 3189–3198

Patel R V., Nahal HK, Breit R, Provart NJ (2012) BAR expressolog identification: Expression profile similarity ranking of homologous genes in plant species. Plant J 71: 1038–1050

Pavlidis P, Gillis J (2012) Progress and challenges in the computational prediction of gene function using networks. F1000Research 1: 2012–2013

Powell AE, Lenhard M (2012) Control of organ size in plants. Curr Biol 22: R360–R367

Pulido P, Spínola MC, Kirchsteiger K, Guinea M, Pascual MB, Sahrawy M, Sandalio LM, Dietz KJ, González M, Cejudo FJ (2010) Functional analysis of the pathways for 2-Cys peroxiredoxin reduction in Arabidopsis thaliana chloroplasts. J Exp Bot 61: 4043–4054

Qin X, Liu JH, Zhao WS, Chen XJ, Guo ZJ, Peng YL (2013) Gibberellin 20-Oxidase Gene OsGA20ox3 regulates plant stature and disease development in rice. Mol Plant-Microbe Interact 26: 227–239

Rhee SY, Mutwil M (2014) Towards revealing the functions of all genes in plants. Trends Plant Sci 19: 212–221

Ruprecht C, Mutwil M, Saxe F, Eder M, Nikoloski Z, Persson S (2011) Large-scale co-expression approach to dissect secondary cell wall formation across plant species. Front Plant Sci 2: 1–

13

Schiffthaler B, Serrano A, Street N, Delhomme N (2018) Seidr: A gene meta-network calculation toolkit. bioRxiv 250696

Schneider M, Gonzalez N, Pauwels L, Inzé D, Baekelandt A (2021) The PEAPOD Pathway and Its Potential To Improve Crop Yield. Trends Plant Sci 26: 220–236

Serin EAR, Nijveen H, Hilhorst HWM, Ligterink W (2016) Learning from co-expression networks: Possibilities and challenges. Front Plant Sci 7: 444

Serrano-Mislata A, Sablowski R (2018) The pillars of land plants: new insights into stem development. Curr Opin Plant Biol 45: 11–17

Simmons CR, Lafitte HR, Reimann KS, Brugière N, Roesler K, Albertsen MC, Greene TW, Habben JE (2021) Successes and insights of an industry biotech program to enhance maize agronomic traits. Plant Sci. doi: 10.1016/j.plantsci.2021.110899

Skirycz A, Radziejwoski A, Busch W, Hannah MA, Czeszejko J, Kwaśniewski M, Zanor MI, Lohmann JU, De Veylder L, Witt I, et al (2008) The DOF transcription factor OBP1 is involved in cell cycle regulation in Arabidopsis thaliana. Plant J 56: 779–792

Soltész A, Vágújfalvi A, Rizza F, Kerepesi I, Galiba G, Cattivelli L, Coraggio I, Crosatti C (2012) The rice Osmyb4 gene enhances tolerance to frost and improves germination under unfavourable conditions in transgenic barley plants. J Appl Genet 53: 133–143

Srivastava AC, Ganesan S, Ismail IO, Ayre BG (2008) Functional characterization of the Arabidopsis AtSUC2 sucrose/H+ symporter by tissue-specific complementation reveals an essential role in phloem loading but not in long-distance transport. Plant Physiol 148: 200–211

Stuart JM, Segal E, Koller D, Kim SK (2003) A gene-coexpression network for global discovery

of conserved genetic modules. Science 302: 249–55.

Sun X, Cahill J, Van Hautegem T, Feys K, Whipple C, Novák O, Delbare S, Versteele C, Demuynck K, De Block J, et al (2017) Altered expression of maize PLASTOCHRON1 enhances biomass and seed yield by extending cell division duration. Nat Commun 8: 14752

Takahashi K, Shimada T, Kondo M, Tamai A, Mori M, Nishimura M, Hara-Nishimura I (2010) Ectopic expression of an esterase, which is a candidate for the unidentified plant cutinase, causes cuticular defects in arabidopsis thaliana. Plant Cell Physiol 51: 123–131

Tanaka T, Ikeda A, Shiojiri K, Ozawa R, Shiki K, Nagai-Kunihiro N, Fujita K, Sugimoto K, Yamato KT, Dohra H, et al (2018) Identification of a hexenal reductase that modulates the composition of green leaf volatiles. Plant Physiol 178: 552–564

Tian Q, Reed JW (1999) Control of auxin-regulated root development by the Arabidopsis thaliana SHY2/AA3 gene. Development 126: 711–721

Tong W, Imai A, Tabata R, Shigenobu S, Yamaguchi K, Yamada M, Hasebe M, Sawa S, Motose H, Takahashi T (2016) Polyamine resistance is increased by mutations in a nitrate transporter gene NRT1.3 (AtNPF6.4) in Arabidopsis thaliana. Front Plant Sci 7: 1–10

Vaishak KP, Yadukrishnan P, Bakshi S, Kushwaha AK, Ramachandran H, Job N, Babu D, Datta S (2019) The B-box bridge between light and hormones in plants. J Photochem Photobiol B Biol 191: 164–174

Van Bel M, Diels T, Vancaester E, Kreft L, Botzki A, Van De Peer Y, Coppens F, Vandepoele K (2018) PLAZA 4.0: An integrative resource for functional, evolutionary and comparative plant genomics. Nucleic Acids Res 46: D1190–D1196

Van Bel M, Proost S, Wischnitzki E, Movahedi S, Scheerlinck C, Van de Peer Y, Vandepoele K (2012) Dissecting plant genomes with the PLAZA comparative genomics platform. Plant Physiol 158: 590–600

966 Vanhaeren H, Nam YJ, De Milde L, Chae E, Storme V, Weigel D, Gonzalez N, Inzé D (2017)
967 Forever young: The role of ubiquitin receptor DA1 and E3 ligase big brother in controlling
968 leaf growth and development. Plant Physiol 173: 1269–1282

969 Verbraeken L, Wuyts N, Mertens S, Cannoot B, Maleux K, Demuynck K, de Block J, Merchie J,
970 Dhondt S, Bonaventure G, et al (2021) Drought affects the rate and duration of organ growth
971 but not inter-organ growth coordination. Plant Physiol 186: 1336–1353

972 Vercruysse J, Baekelandt A, Gonzalez N, Inzé D (2020a) Molecular networks regulating cell
973 division during Arabidopsis leaf growth. J Exp Bot 71: 2365–2378

974 Vercruysse J, Van Bel M, Osuna-Cruz CM, Kulkarni SR, Storme V, Nelissen H, Gonzalez N, Inzé
975 D, Vandepoele K (2020b) Comparative transcriptomics enables the identification of
976 functional orthologous genes involved in early leaf growth. Plant Biotechnol J 18: 553–567

977 Vercruyssen L, Verkest A, Gonzalez N, Heyndrickx KS, Eeckhout D, Han S-K, Jegu T, Archacki
978 R, Van Leene J, Andriankaja M, et al (2014) ANGUSTIFOLIA3 Binds to SWI/SNF
979 Chromatin Remodeling Complexes to Regulate Transcription during Arabidopsis Leaf
980 Development. Plant Cell 26: 210–229

981 Vlad D, Kierzkowski D, Rast MI, Vuolo F, Dello Ioio R, Galinha C, Gan X, Hajheidari M, Hay
982 A, Smith RS, et al (2014) Leaf shape evolution through duplication, regulatory diversification
983 and loss of a homeobox gene. Science 343: 780–783

984 Vuolo F, Kierzkowski D, Runions A, Hajheidari M, Mentink RA, Gupta M Das, Zhang Z, Vlad
985 D, Wang Y, Pecinka A, et al (2018) LMI1 homeodomain protein regulates organ proportions
986 by spatial modulation of endoreduplication. Genes Dev 32: 1361–1366

987 Wolfe CJ, Kohane IS, Butte AJ (2005) Systematic survey reveals general applicability of "guilt-
988 by-association" within gene coexpression networks. BMC Bioinformatics 6: 227

989 Yang X, Lee S, So JH, Dharmasiri S, Dharmasiri N, Ge L, Jensen C, Hangarter R, Hobbie L,

990 Estelle M (2004) The IAA1 protein is encoded by AXR5 and is a substrate of SCF TIR1.
991 Plant J 40: 772–782

992 Zhao J, Favero DS, Peng H, Neff MM (2013) Arabidopsis thaliana AHL family modulates
993 hypocotyl growth redundantly by interacting with each other via the PPC/DUF296 domain.
994 Proc Natl Acad Sci U S A 110: 1–10

995

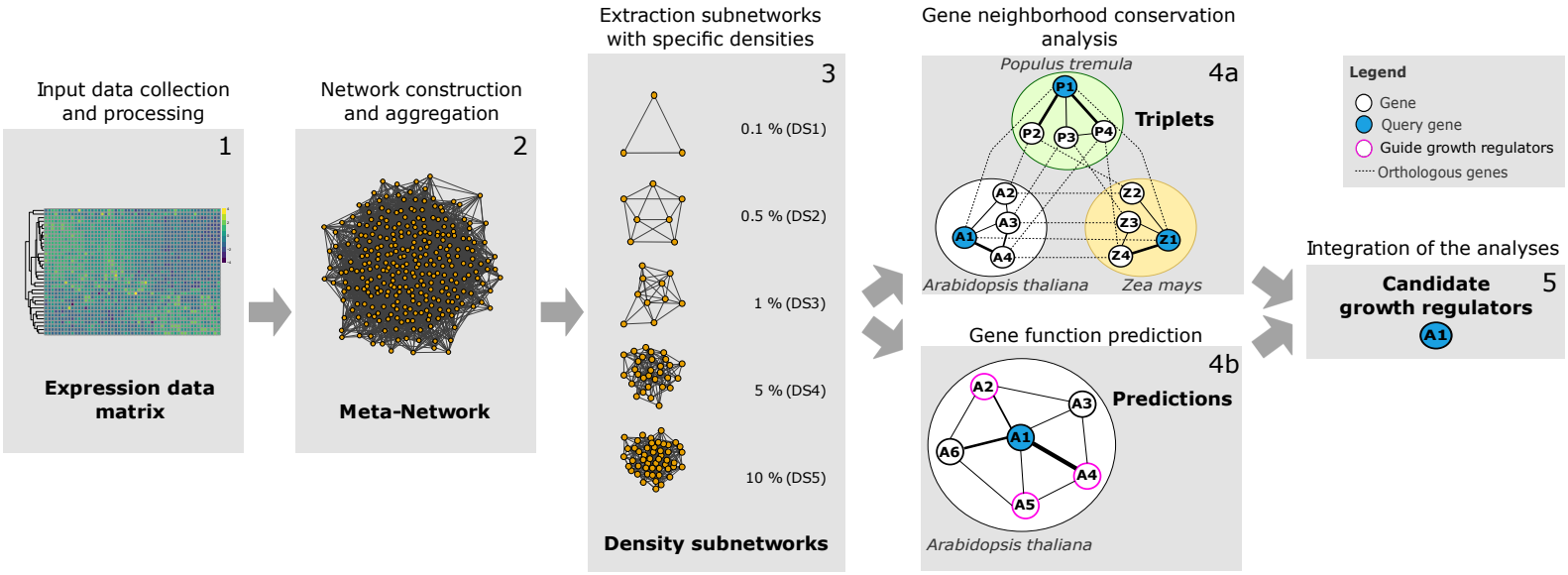


**Figure 1 . Outline of the cross -species network approach to identify candidate growth regulators**. For Arabidopsis, maize and aspen, the expression data (step 1) is used as input to construct a fully connected meta -network per species (step 2). Subsequently , each meta-network is split into five density subnetworks (DSs) by applying specific density cutoffs (step 3). These DSs are the input for two different analyses: they are used first as input to compute cross -species gene neighborhood conservation (step 4a). Secondly, they are used to predict functions via guilt -by-association (step 4b). T his leads to gene function annotations of query genes (blue circles) based on prior knowledge on growth regulators (purple circles). Edge thickness defines in which subnetwork the interaction is conserved (line thickness represents the DS and ranges from 1 , the most stringent DS represented by the thickest line, to 5, the least stringent DS represented by the thinnest line). Finally, the results of these two analyses (steps 4a and 4b) are integrated to obtain a list of candidate growth regulators (step 5).

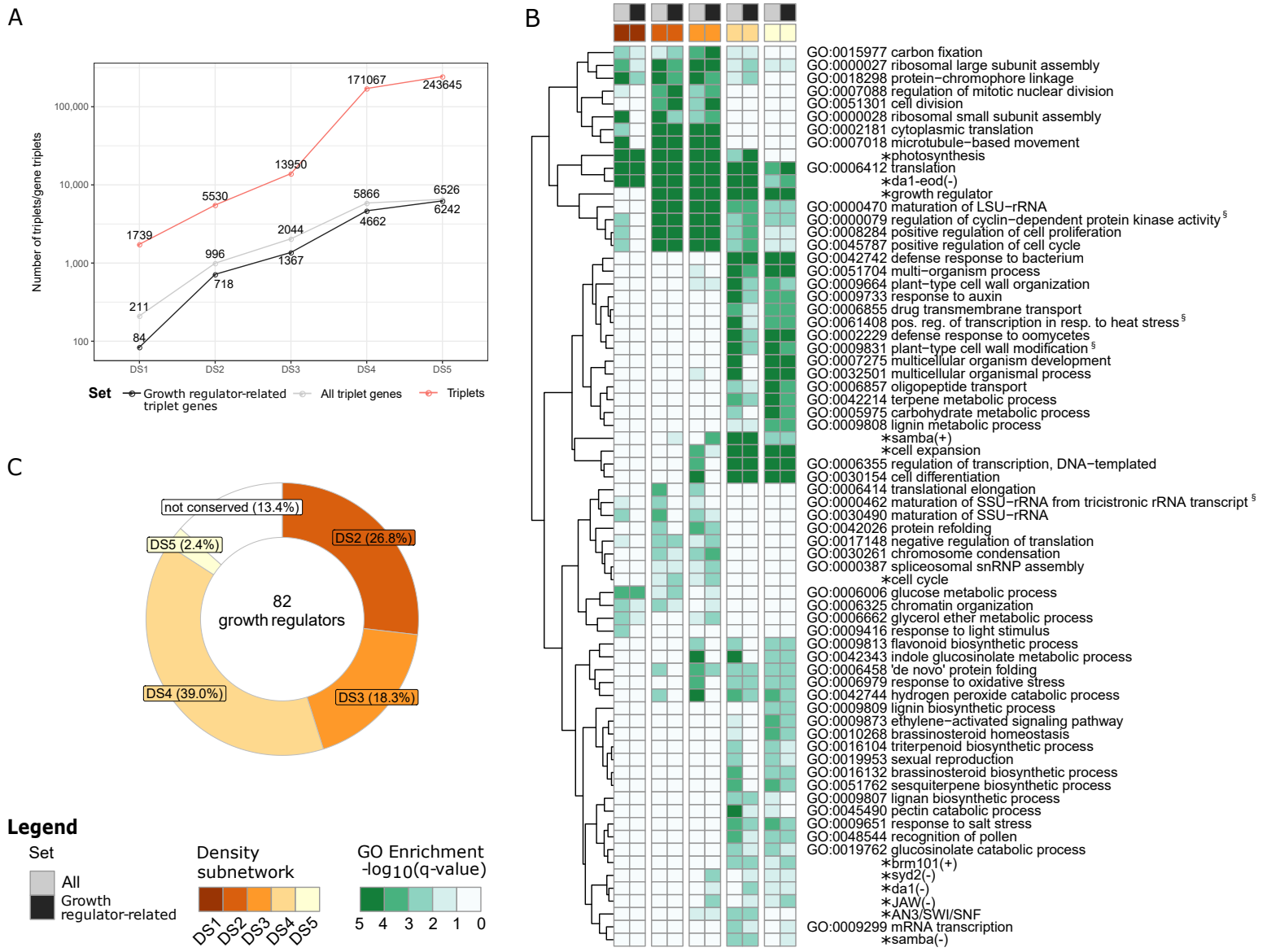


**Figure 2**. **Triplets and their functional enrichments in cross-species conserved leaf networks.** (A) The number of triplet genes showing cross -species gene neighborhood conservation is plotted for all density subnetworks (DSs). (B) The biological process functional over-representation at each DS is summarized for two sets: (1) all triplet genes (All) and (2) growth regulators and their network neighbor (Growth regulator-related) triplet genes, subset of all triplet genes. Functional categories marked with aste risks (*) belong to leaf growth modules described in Vercruysse et al. (2020) and to the differentially expressed gene sets from relevant studies on plant development (Bezhani et al., 2007; Gonzalez et al., 2010; Eloy et al., 2012; Vercruyssen et al., 2014; Vanhaeren et al., 2017). For clarity, long biological process names have been abbreviated (§). (C) Overview of growth regulators with (and without) cross -species neighborhood conservation at different DSs.

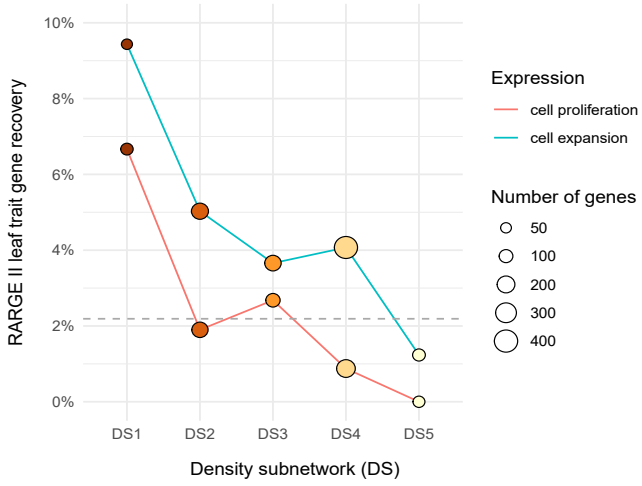


**Figure 3. Recovery of RARGE II leaf trait genes for each density subnetwork split in proliferation and expansion** . The grey dashed line indicates the leaf-related phenotype gene recovery expected by chance (within the RARGE II dataset).

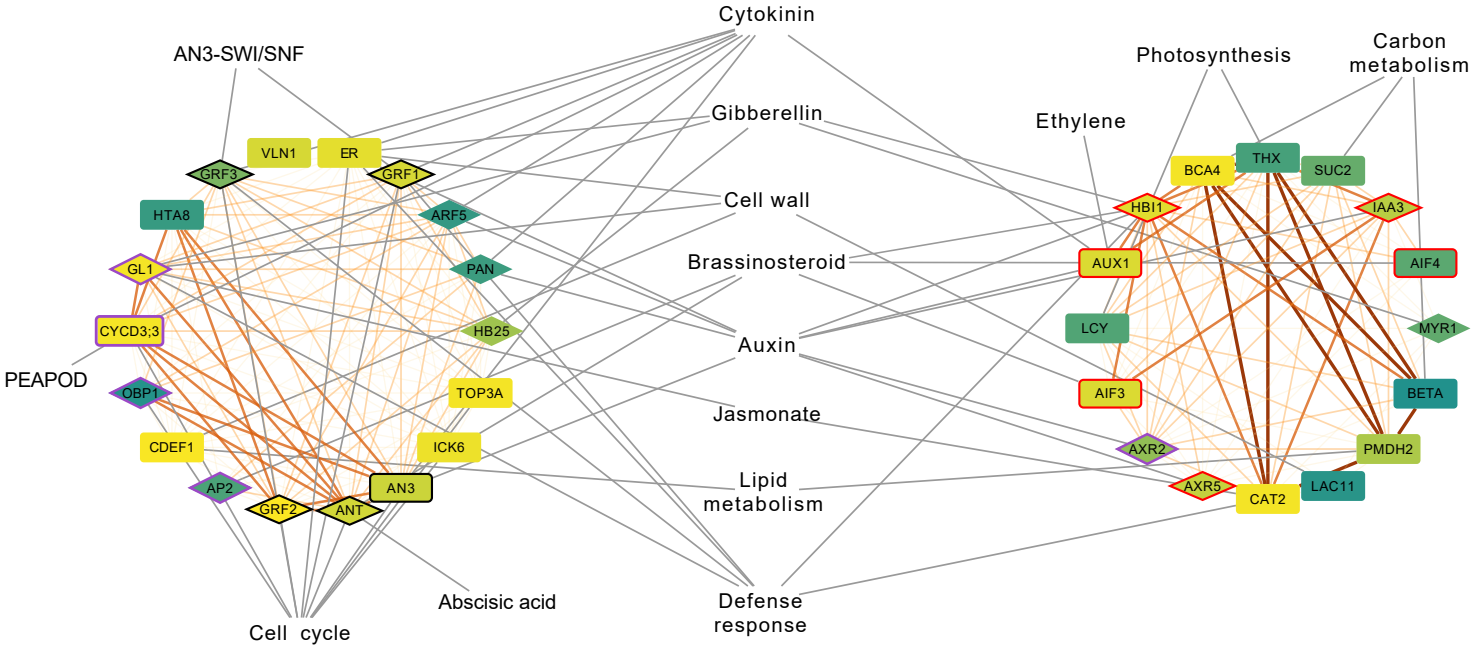


**Figure 4. Gene-function network of the 34 phenotype-related genes out of the top 100 predicted growth regulators**. Predictions are clustered by expression profile (proliferation on the left and expansion on the right). Node label colours from dark green (weak) to yellow (strong) represent the reliability of the gene prediction (GBA score). Node border colours indicate known growth regulators from Arabidopsis (black), known growth regulators from aspen (red), and Arabidopsis known growth regulator paralogs (violet). Diamonds represent transcription factors. Links from dark orange thick (DS1) to light orange thin (DS5) represent the density subnetwork where the genes were found connected. Genes are linked with their respective growth-related pathways (centered if connecting to both proliferation and expansion related genes) by grey links. Anti-correlation links (connecting proliferation with expansion genes) were removed for clarity.

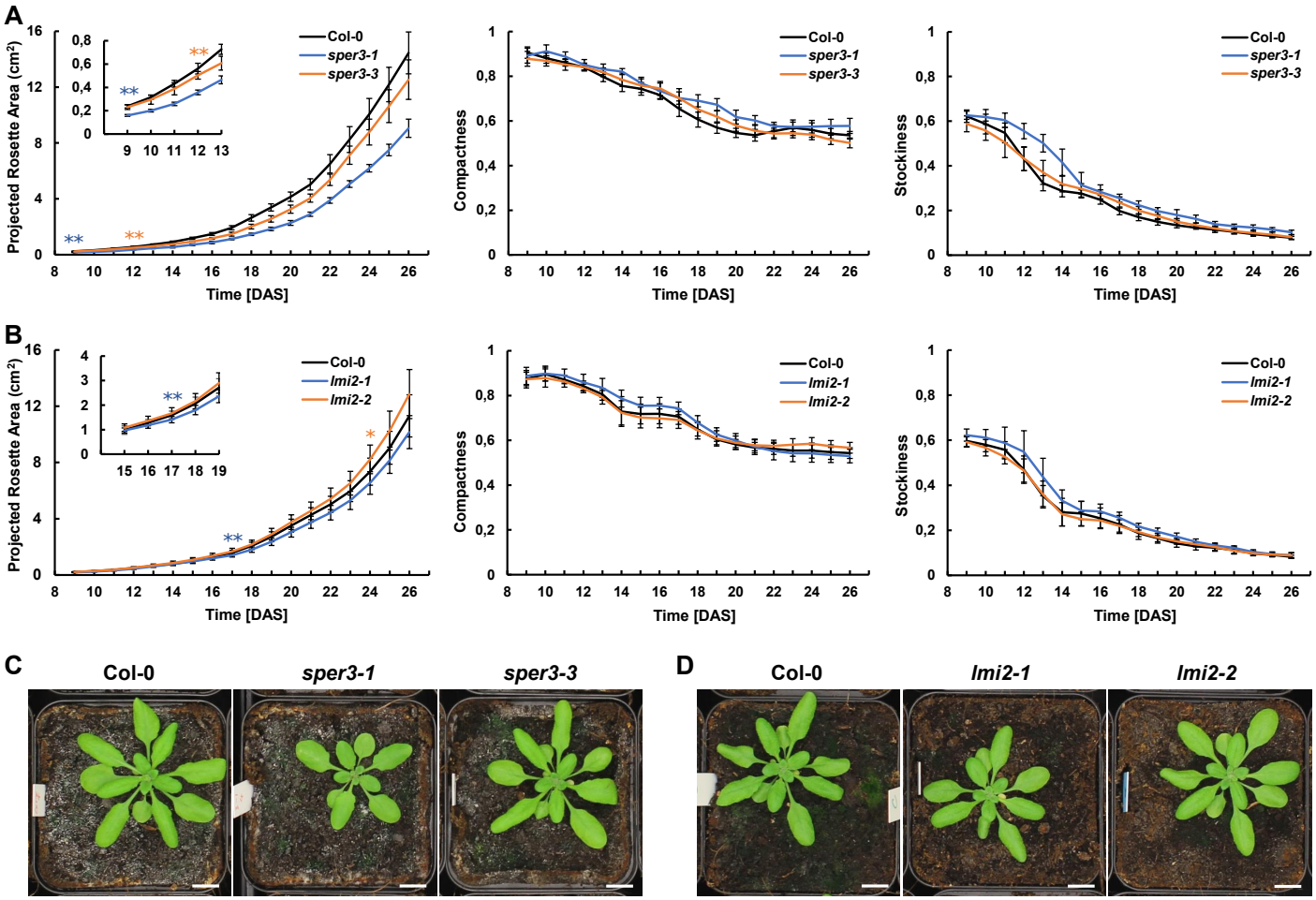


**Figure 5**. **Mutants of predicted growth regulators *NRT1.3* and *LMI2* showed altered rosette growth**. (A-B) Dynamic growth analysis of projected rosette area, compactness and stockiness over time of wild-type Col-0 and the mutants of *NRT1.3* (A) and *LMI2* (B) in soil. Values are means ± SD. For phenotypic analysis of mutants of *LMI2*, sample sizes (n) were n=16 for Col-0, n=16 for *lmi2-2*, and n=17 for *lmi2-1*. For phenotypic analysis of mutants of *NRT1.3*, n=14 for Col-0, n=15 for *sper3-1*, and n=13 for *sper3-3*. The asterisks represent the time points at which differences in the PRA become significant between t he mutants and wild-type, as determined by Student's t test (*, P<0.05; **, P<0.01). The experiments were repeated three times with similar results, and one representative experiment is shown . (C-D) Phenotype of 26-day-old mutants of *NRT1.3* (C) and *LMI2* (D). Scale bar = 1 cm.

# Supplemental Figures: Identification of growth regulators using cross-species network analysis in plants

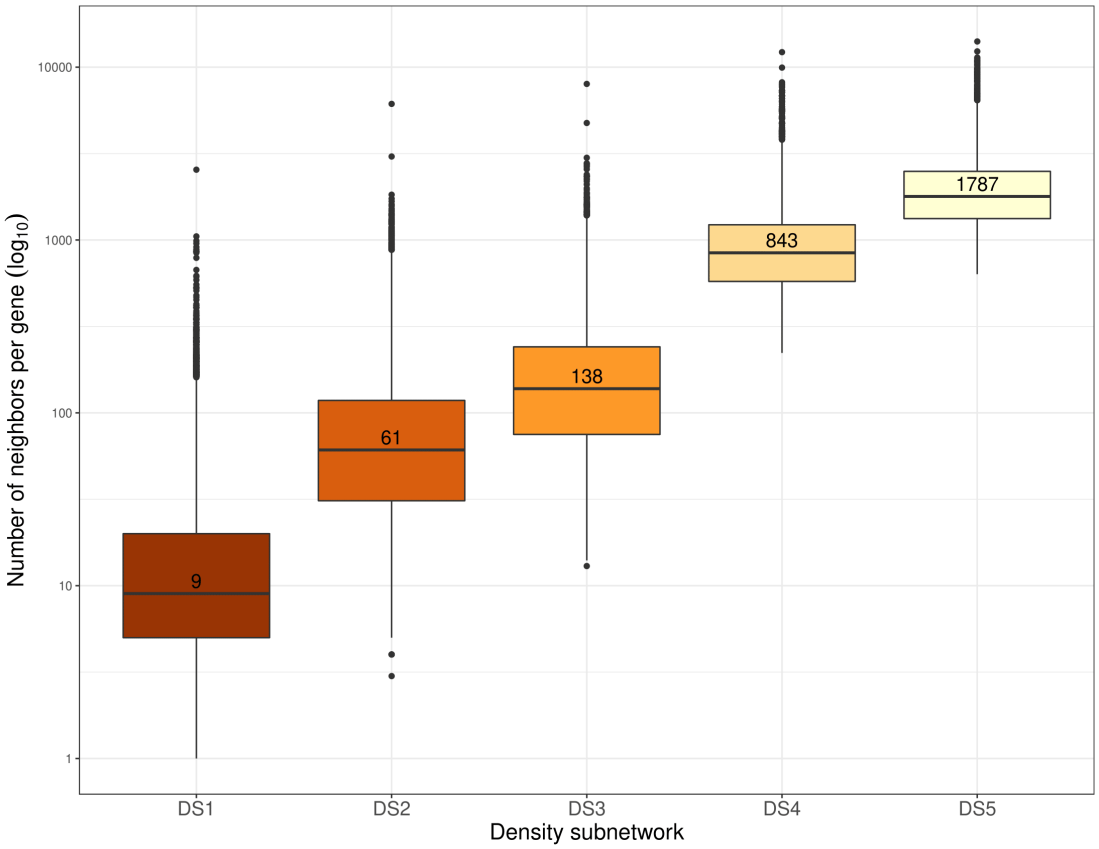


**Supplemental Figure S1**. **Number of neighbors per gene at each density subnetwork in Arabidopsis.** Within each box, horizontal black lines denote median values; boxes extend from the 25th to the 75th percentile of each group's distribution of values; vertical extending lines denote adjacent values (i.e., the most extreme values within 1.5 interquartile range of the 25th and 75th percentile of each group); dots denote observations outside the range of adjacent values. DS refers to density subnetworks.

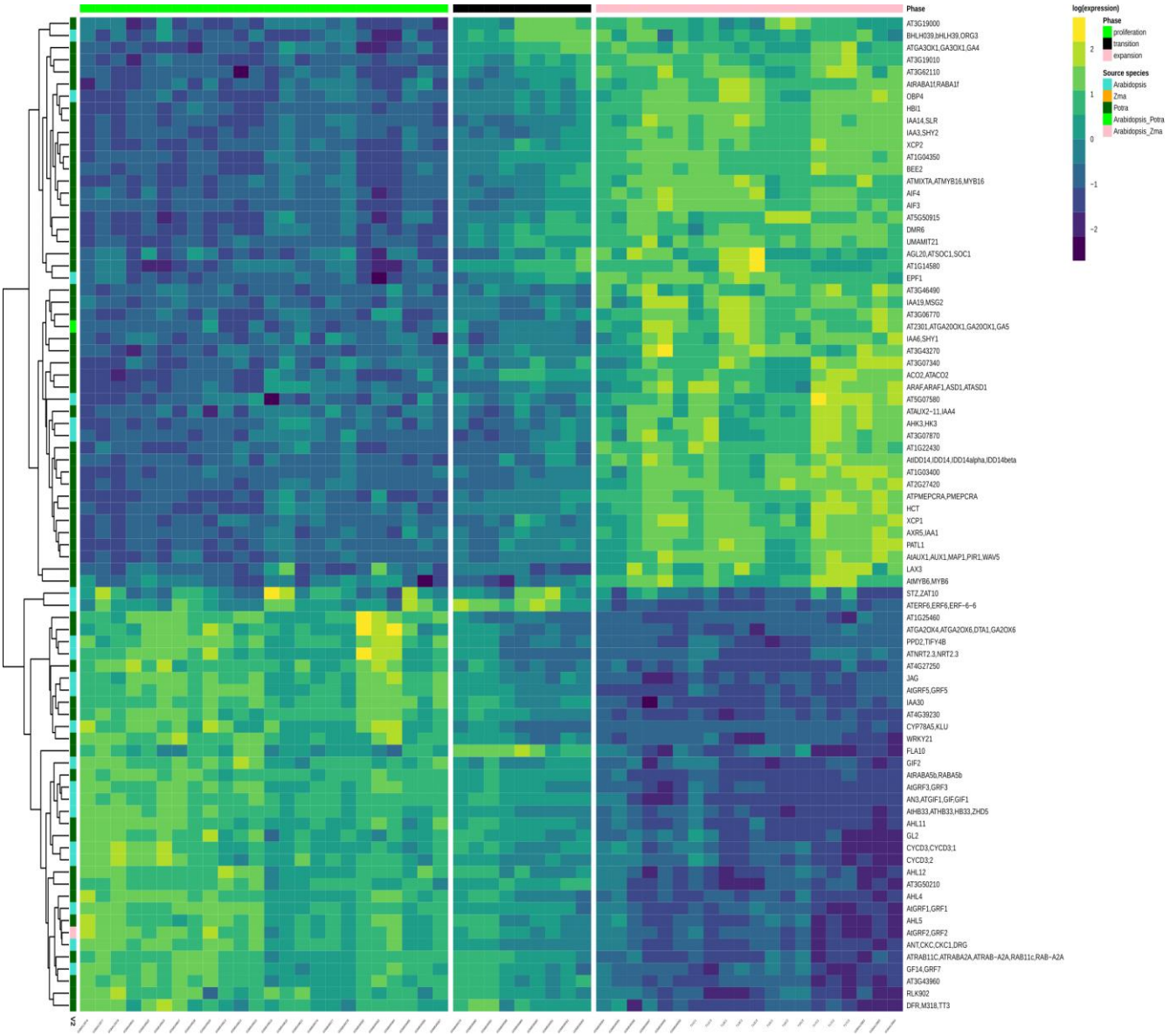


**Supplemental Figure S2**. **Expression patterns for the expression-supported growth regulators in Arabidopsis**. Growth regulator sources are also presented (Arabidopsis, aspen, maize, or shared across two species). Values are row-scaled.

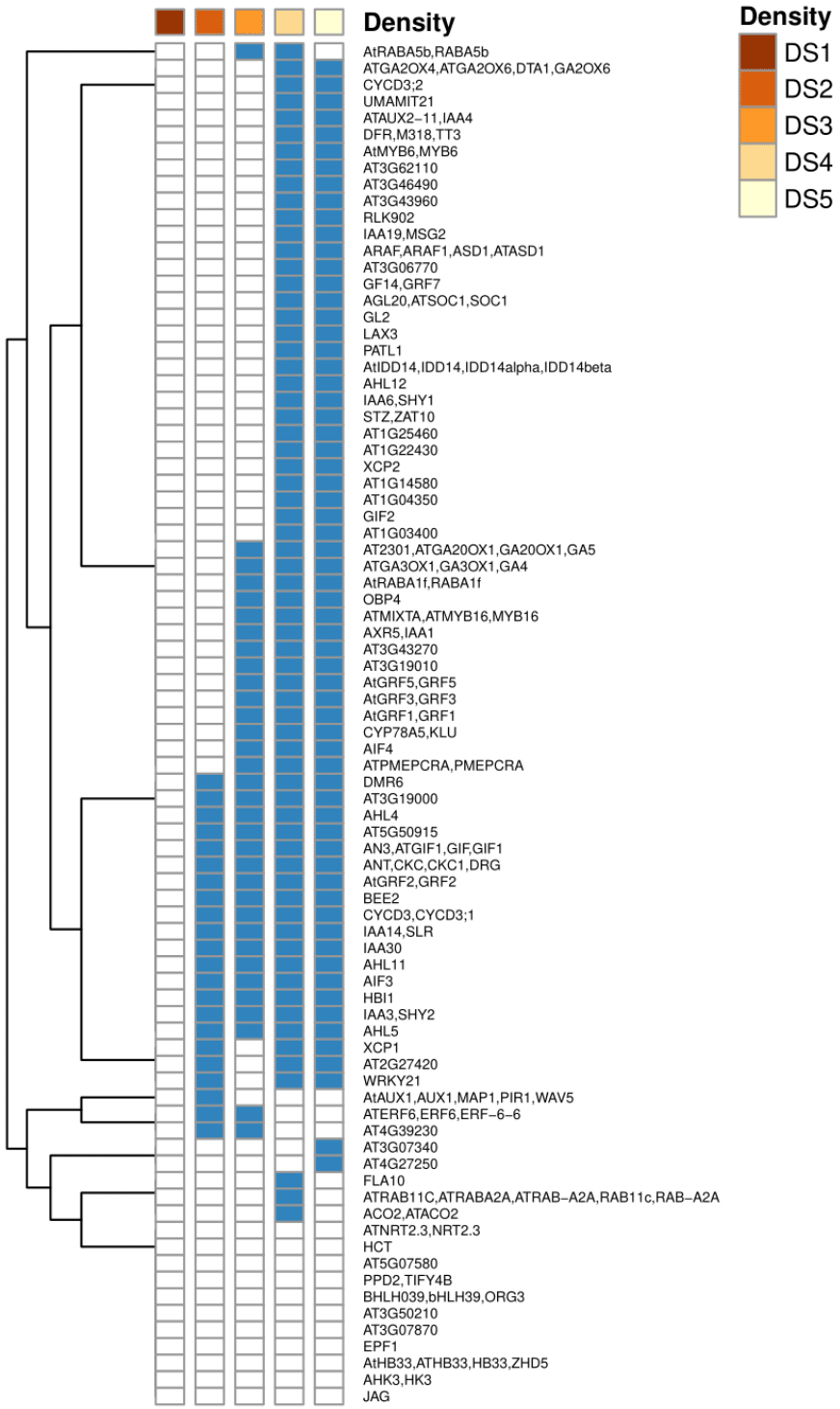


**Supplemental Figure S3**. **Expression-supported growth regulators with neighborhood conservation at each network density level**. DS refers to density subnetworks.

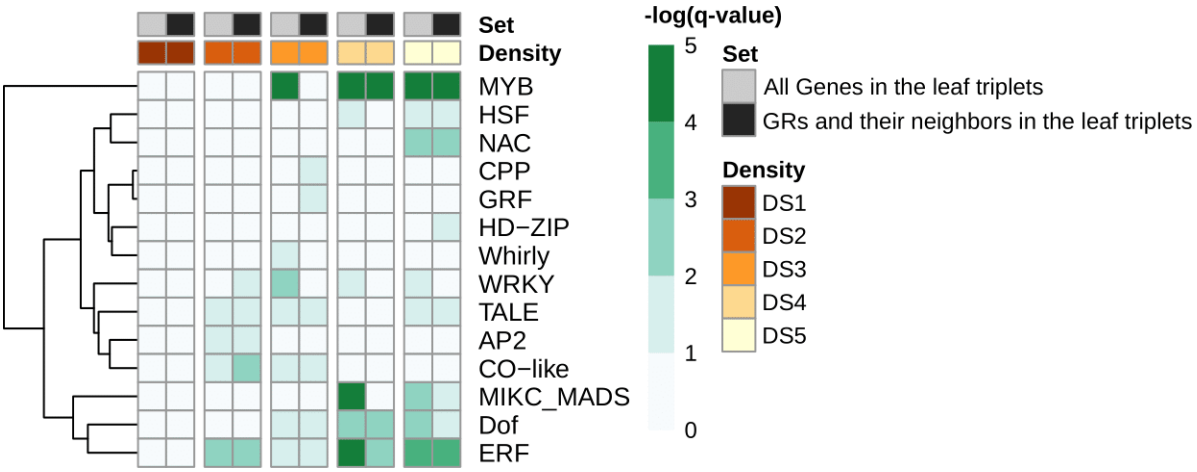


**Supplemental Figure S4**. **Functional enrichment of cross-species conserved transcription factors (TF) grouped by TF family**. Values are expressed as –log(q-value) resulting from the enrichment analysis. DS refers to density subnetworks while GR refer to growth regulators.

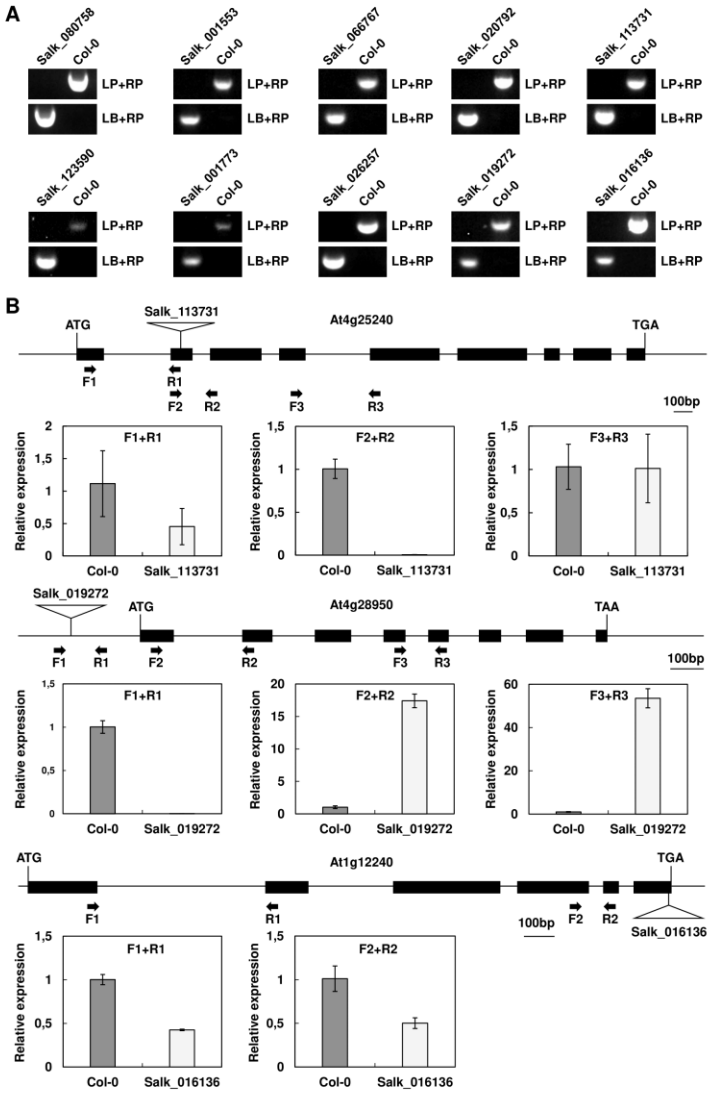


**Supplemental Figure S5. Identification of T-DNA insertion lines.** (A) Molecular analysis of T-DNA insertion lines by PCR using a T-DNA primer and gene-specific primers. (B) Quantitative real-time PCR analysis showed the disrupted expression of At4g25240 in Salk_113731, the increased expression of At4g28950 in Salk_019272, and the decreased expression of At1g12240 in Salk_016136, respectively. The data represent means ± SD calculated from three biological replicates. LP, left primer; RP, right primer; LB, left border primer; F1 ,F2, F3, forward primers; R1, R2, R3, reverse primers.

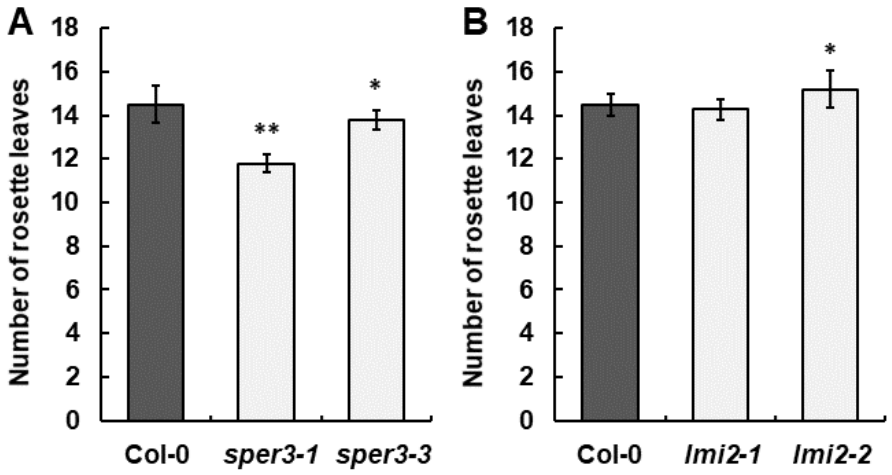


**Supplemental Figure S6. The rosette leaf numbers of the wild-type Col-0 and the mutants of *NRT1.3* and *LMI2*.** The rosette leaf number of 26-day-old wild-type Col-0 and the mutants of *NRT1.3* (A) and *LMI2* (B). Asterisks denote significant differences compared to the wild-type Col-0, as determined by Student's *t* test (*, $P<0.05$; **, $P<0.01$).

## Supplemental Methods

### Maize developmental expression dataset

### Maize growth conditions

Maize plants were grown in growth chambers with controlled relative humidity (55%), temperature (24 °C day/18 °C night), and light intensity (170–200 μmol $m^{-2}$ $s^{-1}$ photosynthetic active radiation at plant level) provided by a combination of high-pressure sodium vapor (RNP-T/LR/400W/S/230/E40; Radium) and metal halide lamps with quartz burners (HRI-BT/400W/D230/E40; Radium) in a 16-h/8-h (day/night) cycle.

### Developmental maize compendium (15 samples)

Three sections (from the base to 3.5 cm, from 3.5 to 7.0 cm and from 7.0 to 10.5 cm) of a developing leaf 4 were harvested two days after leaf emergence, from maize B104 inbred plants. To aim for enough tissue per section and per replicate, 28 plants per replicate were pooled. In total, five biological replicates for the three sections (15 samples in total) were used for RNAseq. After harvesting, samples were directly frozen in liquid nitrogen. Total RNA was extracted using the guanidinium thiocyanate-phenol-chloroform extraction method using TRI-reagent (Thermo Fisher Scientific) followed by DNA digestion using the RQ1 RNase-free DNase kit (Promega). Total RNA was sent to GATC Biotech for RNA sequencing. Library preparation was done using the NEBNext Kit (Illumina). In brief, purified poly(A)-containing mRNA molecules were fragmented, randomly primed strand-specific cDNA was generated and adapters were ligated. After quality control using an Advanced Analytical Technologies Fragment Analyzer, clusters were generated through amplification using cBOT (Cluster Kit v4, Illumina), followed by sequencing on an Illumina Hi Seq2500 with the TruSeq SBS Kit v3 (Illumina). Sequencing was performed in paired-end mode with a read length of 125 nt.

### Quantitative real-time PCR (qPCR) for zone delineation in the developmental maize compendium (methods)

The first ten cm of a growing fourth leaf, two days after leaf emergence, from maize B104 inbred lines was harvested and segmented into smaller pieces of 5mm (basal two cm) and 10mm (distal eight cm). For each piece, we had three biological replicates, each pool consisting of tissue of three plants. After harvesting, samples were directly frozen in liquid nitrogen. Total RNA was extracted

using the guanidinium thiocyanate-phenol-chloroform extraction method using TRI-reagent (Thermo Fisher Scientific) followed by DNA digestion using the RQ1 RNase-free DNase kit (Promega). cDNA was prepared from 1 µg of total RNA with the iScript cDNA Synthesis Kit (Biorad). The qPCR was done on a Lightcycler 480 (Roche) with SYBR green for detection in a 5-µl volume (2,5 µl of mastermix, 0,25 µl of 5 µM of each forward and reverse primer and 2 µl of cDNA). Every reaction was performed in triplicate on a 384-multiwell plate to allow determination of mean and SEM of cycle threshold (CT) values. Data were analyzed in Microsoft Excel with the 2-ΔΔCT method (Schmittgen and Livak, 2008) and values were standardized against those of 18S rRNA (primers P1 and P2). The mean expression levels were calculated from three biological repeats, using the P3 and P4 primers for phosphoribulokinase, P5 and P6 for NADP malate dehydrogenase, P7 and P8 for NADP-malic enzyme (NADP-ME), P9 and P10 for Photosystem Q(B) protein (psbA), P11 and P12 for cytochrome B6 (petB), P13 and P14 for NADPH-quinone oxidoreductase subunit 1 (ndhA), P15 and P16 for Photosystem I iron-sulfur center (psaC) and P17 and P18 for phosphoenolpyruvate carboxylase (PEPC) (**Supplemental Methods Figure 1**).

**qPCR for zone delineation in the developmental maize compendium (assay results)**

Throughout the developmental gradient represented in the maize leaf growth zone, genes related to photosynthesis are differentially expressed, some even starting in the division zone and expansion zone (Nelissen et al., 2018). Therefore, the maize RNAseq compendium along the developmental gradient of a growing maize leaf three zones were delineated based on a qPCR analysis of several known genes involved in photosynthesis (Wang et al., 2014; Chotewutmontri and Barkan, 2016; Schlüter and Weber, 2019; Heldt and Piechulla, 2021). The qPCR results showed that those genes had specific transcriptional profiles in the lower half of maize leaves that can be divided in three classes. The fragment from the base to 3.5 cm, contains the leaf growth zone in which only the tested transcripts involved in the light dependent reactions of photosystem I and II (Photosystem Q(B) protein (psbA), cytochrome B6 (petB), NADPH-quinone oxidoreductase subunit 1 (ndhA) and Photosystem I iron-sulfur center (psaC)) were expressed (**Supplemental Methods Figure 1**). Their expression gradually increased along the leaf developmental gradient. The expression level of the other tested genes involved in the C4 carbon assimilation cycle was minimal at the base of the leaf and their transcription levels started to increase from 3.5 to 7.0 cm (NADP malate dehydrogenase and phosphoenolpyruvate carboxylase

(PEPC)) or even only started to show an increase in expression in the mature part of the leaf from 7.0 to 10.5 cm (NADP-malic enzyme (NADP-ME) and phosphoribulokinase) (**Supplemental Methods Figure 1**). From 7.0 to 10.5 cm the expression of all genes had reached their maximal value.

In conclusion, based on a qPCR analysis of genes involved in photosynthesis, three zones along the developmental gradient of the maize leaf were harvested. While the first section consisted of proliferative and expanding leaf tissue (base to 3.5 cm), the second section (3.5 to 7.0 cm) contained expanding and mature cells and the last part (7.0 to 10.5 cm) was fully mature.

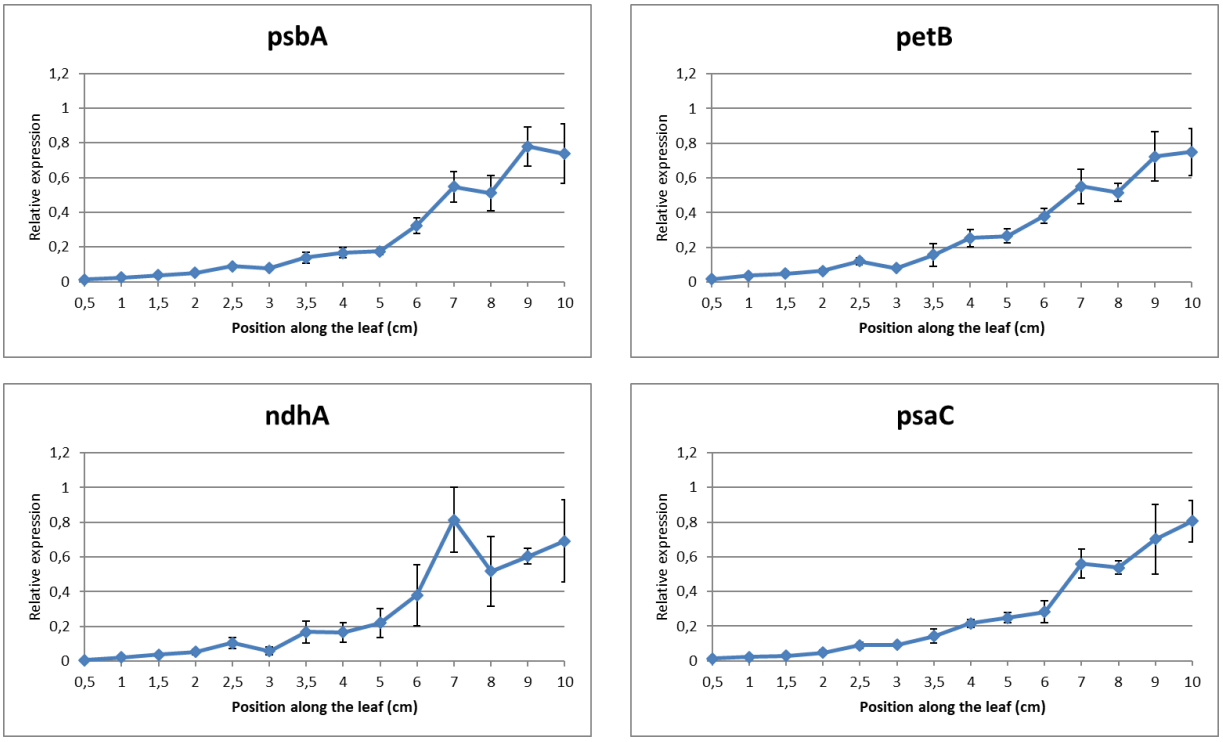

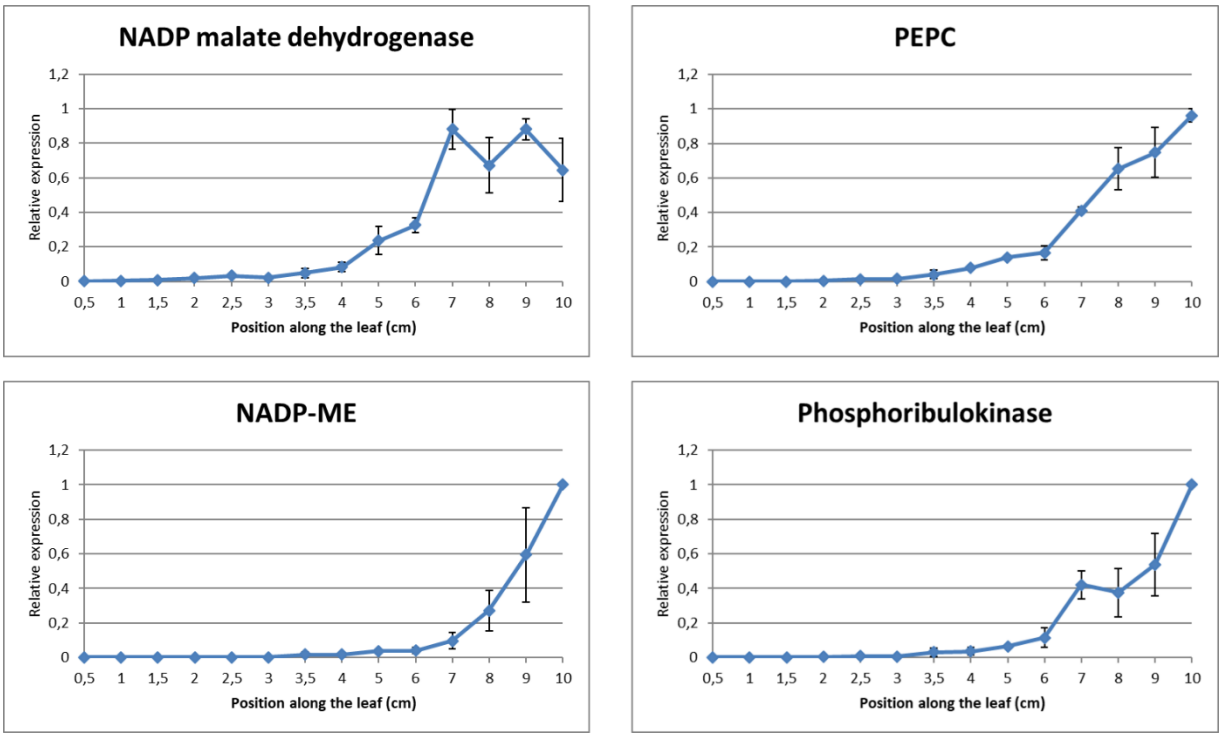


**Supplemental Methods Figure 1.** Transcripts encoding critical C4 photosynthesis enzymes are differentially expressed in a gradient fashion in the lower half of B104 maize leaves.

**Proliferative maize samples (3 samples)**

The three proliferative maize dataset samples were taken from the inbred line B104. The first basal half cm (dividing cells) of leaf four two days after leaf appearance was sampled. Three biological replicates were taken, each pool consisting of proliferative tissue of three plants. After harvesting, samples were directly frozen in liquid nitrogen. Total RNA was extracted using the guanidinium thiocyanate-phenol-chloroform extraction method using TRI-reagent (Sigma-Aldrich). RNA concentration and purity were determined spectrophotometrically using the Nanodrop ND-1000 (Nanodrop Technologies) and RNA integrity was assessed using a Bioanalyser 2100 (Agilent). Per sample, 500 ng of total RNA was used as input. Using the Illumina TruSeq® Stranded mRNA Sample Prep Kit (protocol 15031047 Rev E October 2013) poly-A containing mRNA molecules were purified from the total RNA input using poly-T oligo-attached magnetic beads. In a reverse transcription reaction using random primers, RNA was converted into first strand cDNA and subsequently converted into double-stranded cDNA in a second strand cDNA synthesis reaction. The cDNA fragments were extended with a single 'A' base to the 3' ends of the blunt-ended cDNA

fragments after which multiple indexing adapters were ligated introducing different barcodes for each sample. Finally, enrichment PCR was carried out to enrich those DNA fragments that have adapter molecules on both ends and to amplify the amount of DNA in the library. For the sequence run, libraries were equimolarly pooled and sequenced using a high 300 cycles (PE- 2 x 150 bp) NextSeq kit. Sequencing was performed on an Illumina NextSeq 500 Paired-End mode.

**Other maize samples (6 samples)**

Other six maize samples corresponding to proliferation stage of developing leaf 4 were obtained from Sun et al. (2017) (see the original article for more details).

**Maize data processing**

The 24 total RNA-seq sample reads were processed with Prose (Vaneechoutte and Vandepoele, 2019), which implements kallisto (Bray et al., 2016) for mapping against the maize genome version B73 RefGen_v3.

**Aspen developmental expression dataset (see the original article for more details)**

Aspen data was obtained by the developmental series of terminal leaves published by (Mähler et al., 2020) (LeafDev dataset, 33 samples). This dataset was composed by: the first fully unfurled leaf, defined as a reference point and labeled leaf T0; three leaves above the reference leaf (labeled as T-1, T-2, and T-3) and the apical region, containing the shoot apical meristem; the very youngest leaf primordia (labeled T-4); and two leaves below the reference leaf (labeled T1 and T2).

**Arabidopsis developmental expression dataset (see the original articles for more details)**

Transcriptomic data for Arabidopsis were obtained from several studies: AGRONOMICS1 Tilling Array (Andriankaja et al., 2012) including leaves from seedlings harvested at the stages of proliferation (8 and 9 days after sowing (DAS)), transition (10, 11, and 12 DAS), and expansion (13 and 14 DAS) for a total of 24 samples; ATH1-array (Skirycz et al., 2010) including leaves harvested from plants at proliferation (9 DAS) and expansion (15 DAS) stages for a total of 6 samples. ATH1-array (Skirycz et al., 2011) including leaves harvested at proliferation stage (9 DAS). RNA-seq data (Dubois et al., 2017) including leaves harvested at expansion stage (11 DAS) for a total of 11 samples.

**Arabidopsis data processing**

The integration of array and RNA-seq data followed two main steps. The first was performed to obtain two datasets with the same distribution and was performed via the quantile normalization selecting processed RNA-seq data sample-set (11 samples) as target distribution and microarray sample-set (42 samples) as reference distribution (Thompson et al., 2016). In the second step, all samples were inspected using principal component analysis (PCA). Batch effect correction was applied using ComBat implemented in the R package SVA to remove non-biological sources of variation in the dataset (Leek et al., 2010).

**References**


Andriankaja M, Dhondt S, De Bodt S, Vanhaeren H, Coppens F, De Milde L, Mü hlenbock P, Skirycz A, Gonzalez N, Beemster GT, et al (2012) Exit from Proliferation during Leaf Development in Arabidopsis thaliana: A Not-So-Gradual Process. Dev Cell 22: 64–78

Bray NL, Pimentel H, Melsted P, Pachter L (2016) Near-optimal probabilistic RNA-seq quantification. Nat Biotechnol 34: 525–527

Chotewutmontri P, Barkan A (2016) Dynamics of Chloroplast Translation during Chloroplast Differentiation in Maize. PLoS Genet 12: 1–28

Dubois M, Claeys H, Van den Broeck L, Inzé D (2017) Time of day determines Arabidopsis transcriptome and growth dynamics under mild drought. Plant Cell Environ 40: 180–189

Heldt HW, Piechulla B (2021) Photosynthesis needs the consumption of water. Plant Biochemistry (Fifth edition): 191-216

Leek JT, Scharpf RB, Bravo HC, Simcha D, Langmead B, Johnson WE, Geman D, Baggerly K, Irizarry RA (2010) Tackling the widespread and critical impact of batch effects in high-throughput data. Nat Rev Genet 11: 733–739

Mähler N, Schiffthaler B, Robinson KM, Terebieniec BK, Vučak M, Mannapperuma C, Bailey MES, Jansson S, Hvidsten TR, Street NR (2020) Leaf shape in Populus tremula is a complex, omnigenic trait. Ecol Evol 10: 11922–11940

Nelissen H, Sun XH, Rymen B, Jikumaru Y, Kojima M, Takebayashi Y, Abbeloos R, Demuynck

K, Storme V, Vuylsteke M, et al (2018) The reduction in maize leaf growth under mild drought affects the transition between cell division and cell expansion and cannot be restored by elevated gibberellic acid levels. Plant Biotechnol J 16: 615–627

Schlüter U, Weber A (2019) Regulation and Evolution of C4 Photosynthesis. FASEB J 33: 183–215

Schmittgen TD, Livak KJ (2008) Analyzing real-time PCR data by the comparative CT method. Nat Protoc 3: 1101–1108

Skirycz A, De Bodt S, Obata T, De Clercq I, Claeys H, De Rycke R, Andriankaja M, Van Aken O, Van Breusegem F, Fernie AR, et al (2010) Developmental Stage Specificity and the Role of Mitochondrial Metabolism in the Response of Arabidopsis Leaves to Prolonged Mild Osmotic Stress. Plant Physiol 152: 226–244

Skirycz A, Claeys H, De Bodt S, Oikawa A, Shinoda S, Andriankaja M, Maleux K, Eloy NB, Coppens F, Yoo S-D, et al (2011) Pause-and-Stop: The Effects of Osmotic Stress on Cell Proliferation during Early Leaf Development in *Arabidopsis* and a Role for Ethylene Signaling in Cell Cycle Arrest. Plant Cell 23: 1876–1888

Sun X, Cahill J, Van Hautegem T, Feys K, Whipple C, Novák O, Delbare S, Versteele C, Demuynck K, De Block J, et al (2017) Altered expression of maize PLASTOCHRON1 enhances biomass and seed yield by extending cell division duration. Nat Commun 8: 14752

Thompson JA, Tan J, Greene CS (2016) Cross-platform normalization of microarray and RNA-seq data for machine learning applications. PeerJ 4: e1621

Vaneechoutte D, Vandepoele K (2019) Curse: Building expression atlases and co-expression networks from public RNA-Seq data. Bioinformatics 35: 2880–2881

Wang Y, Long SP, Zhu XG (2014) Elements required for an efficient NADP-malic enzyme type C4 photosynthesis. Plant Physiol 164: 2231–2246